Porous Inorganic Materials

Xiqing Wang,[2] Xianhui Bu[1] & Pingyun Feng[2]
[1] *California State University, Long Beach, CA, USA*
[2] *University of California Riverside, Riverside, CA, USA*

Glossary

M41S: A family of mesoporous materials including MCM-41, MCM-48, and MCM-50
MSU-1,2,3,4: Michigan State University no. 1, 2, 3, 4, a series of wormhole mesoporous materials prepared in the presence of nonionic surfactants
Pluronic: polyethylene oxide–polypropylene oxide triblock surfactant, $(EO)_m(PO)_n(EO)_m$, for example, P123 = $(EO)_{20}(PO)_{70}(EO)_{20}$
SBA-x: Santa Barbara no. x, a series of mesoporous materials
Tergitol: alkyl–polyethylene oxide surfactant, $C_nH_{2n+1}(EO)_m$
Triton-X: alkylaryl–polyethyleneoxide surfactant, $C_nH_{2n+1}Ph(EO)_m$

Abbreviations

2D or 3D = 2 or 3 dimensional; 3DOM = 3-dimensional ordered macroporous materials; CMK-1,2, 3 = Carbon mesostructured by KAIST (Korea Advanced Institute of Science and Technology) no. 1, 2, 3; CTAB = Cetyltrimethylammonium bromide, $[C_{16}H_{33}N(CH_3)_3]^+Br^-$; HMS = Hexagonal molecular sieves. ICF-m = Inorganic chalcogenide framework, no. m; MCF = Mesostructured cellular foams; MCM-41, 48, 50 = Mobil composition of matter no. 41, 48, and 50; MMS = Mesoporous molecular sieves; PCH = porous clay heterostructures; SEM = Scanning electron microscopy; TEM = Transmission electron microscopy; TEOS = Tetraethoxysilane.

1 INTRODUCTION

Porous materials are of great interest because of their wide commercial applications as ion exchangers, adsorbents, and catalysts. There are a variety of porous materials differing in chemical composition, pore geometry and size, and degree of crystallinity. According to the IUPAC definition,[1] porous materials are classified into three groups on the basis of pore size: microporous materials are porous solids with pore size below 2 nm, mesoporous materials are porous solids with pore size between 2 and 50 nm, and macroporous materials are those with pore size larger than 50 nm (Figure 1).

Pores with different sizes show characteristic physical adsorption effects as manifested in the isotherm.[2] The isotherm shows the relationship between the amount of a given gas taken up or released by a solid as a function of the gas pressure under a constant temperature. The type-I isotherm shows a steep increase at very low pressures and a long saturation plateau and is characteristic of microporous materials. The type-IV isotherm exhibits a steep increase at high relative pressure and, in many cases, a hysteresis loop, which is associated with capillary condensation in mesopores.

The development of microporous materials started in late 1940s with the synthesis of synthetic zeolites by Barrer, Milton, Breck, and their coworkers. Some commercially important microporous materials such as zeolites A, X, and Y were made in the first several years of Milton and Breck's work. In the following 30 years, zeolites with various topologies and chemical compositions were prepared, culminating in the synthesis of ZSM-5 and its aluminum-free pure silica form in 1970s. A breakthrough leading to an extension of crystalline microporous materials to nonsilicates occurred in 1982 when Flanigen *et al*. reported the synthesis of aluminophosphate molecular sieves. Since the late 1980s and the early 1990s, crystalline microporous materials have been made in many other compositions including chalcogenides and metal–organic frameworks.

Prior to the 1990s, materials with pore size in the meso range such as silica gels and activated carbons show disordered pore structure with a broad distribution of pore size. In 1992, by using cationic surfactants as template, Mobil scientists

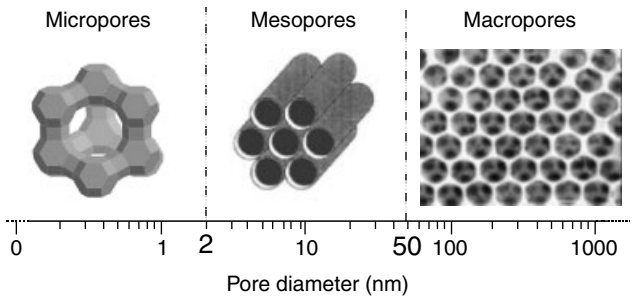

Figure 1 The IUPAC classification of porous materials on the basis of pore diameter

Encyclopedia of Inorganic and Bioinorganic Chemistry, Online © 2011 John Wiley & Sons, Ltd.

This article was originally published in the *Encyclopedia of Inorganic Chemistry* in 2006 by John Wiley & Sons, Ltd.
DOI: 10.1002/9781119951438.eibc0264

prepared a family of mesoporous silicas (denoted M41S) with hexagonal and cubic symmetry and highly uniform pore sizes ranging from 2 to 10 nm. There has been a widespread interest in ordered mesoporous materials since the discovery of M41S.

Following the discovery of ordered mesoporous materials, the templated approach was also employed for the synthesis of ordered macroporous materials. Macroporous materials with uniform pore sizes are predicted to have useful optical properties and may have applications as photonic crystals with optical band gaps.[3]

This article focuses on ordered mesoporous materials that have undergone a rapid growth in the past decade. For completeness, the concurrent progresses in the areas of crystalline microporous and ordered macroporous materials are briefly described.

2 MICROPOROUS MATERIALS[4]

Microporous materials are formed with hydrated inorganic cations or organic species located within cavities of the extended inorganic or inorganic–organic hybrid host framework. Extra-framework organic species are usually protonated amines, quaternary ammonium cations, or neutral solvent molecules. Dehydration (or desolvation) and calcination are two methods frequently used to remove extra-framework species and generate microporosity.

Even though crystalline microporous materials include those with pore size between 10 and 20 Å (called extra-large pore materials), few of them have a pore size within this range. This limits the applications of microporous materials to small molecules. There has always been a desire to increase the pore size of a crystalline material to more than 10 Å while maintaining adequate thermal or hydrothermal stability required for various applications.[5] Recent advances in chalcogenide and metal–organic framework materials have shown much promise for the preparation of extra-large pore materials.

In addition to the desire for an increase in the pore size, there has been a strong interest in generating multifunctional materials in which crystalline microporosity is integrated with other useful properties such as framework chirality, ferromagnetism, semiconductivity, or ion conductivity.[6]

2.1 Microporous Silicates and Germanates

Microporous materials are typified by natural and synthetic zeolites that are crystalline 3D aluminosilicates with open channels or cages. Synthetic and structural concepts of zeolites have to a large extent shaped the development of microporous materials during the past 50 years. For example, the use of organic structure-directing agents in the synthesis of high-silica zeolites and their all-silica polymorphs contributed to the later discovery of aluminophosphate molecular sieves. A comprehensive review on the synthesis and structure of zeolites and related materials has been given by Dyer and will not be repeated here.[7]

The commercial importance of zeolites has prompted numerous efforts aimed at the synthesis of new microporous materials. One commonly used approach is through the substitution of framework cations (i.e. Al^{3+} or Si^{4+}) in zeolites by other cations such as Ga^{3+}, Ge^{4+}, and P^{5+}. Because of the close resemblance to zeolites, gallosilicates and alumino- (or gallo-) germanates were among the earliest nonzeolite microporous materials being prepared. In general, gallosilicates and alumino- (or gallo-) germanates do not possess framework topologies not previously found among zeolites. However, the recent use of organic structure-directing agents in the synthesis of germanates has resulted in a number of materials with unprecedented framework topologies.[8]

In general, each compositional system has a unique range of the T–O bond length and the T–O–T angle (where T refers to tetrahedral atoms) and has its own preference for certain types of framework topology. For example, structures with strained double four-ring units are more likely to occur as germanates. Another example is the synthesis of UCSB-7. It could be prepared under a variety of experimental conditions as either a gallogermanate or aluminogermanate.[9] However, it has not been prepared as a silicate. It is thus not surprising to find that by incorporating the germanium source into the synthesis mixture of silicates, new microporous materials could be synthesized.[10]

2.2 Microporous Phosphates and Arsenates[11]

The synthesis of aluminophosphate molecular sieves in 1980s represents a breakthrough in the development of microporous materials. Since then, much of the worldwide synthetic efforts have been directed toward nonsilicate microporous materials. Many novel framework topologies could be found with phosphates, and many other elements could be incorporated into phosphates to produce additional new framework topologies or new compositions.

Aluminophosphate molecular sieves, as originally prepared, have a neutral framework and generally require organic amines or alkylammonium cations as extra-framework species. However, it was soon discovered that both Si^{4+} and many metal cations (in particular divalent metal cations) could be incorporated into the aluminophosphate framework to generate a negative framework similar to high-silica zeolites. A complete substitution of Al^{3+} sites by divalent cations such as Zn^{2+} or Be^{2+} gives a series of zinco- or beryllo-phosphates that are similar to low-silica zeolites. The negative framework charge and the associated extra-framework charge-balancing cations are useful for many applications of microporous materials; however, the stability of microporous materials generally decreases with increasing negative charge on the framework.

Encyclopedia of Inorganic and Bioinorganic Chemistry, Online © 2011 John Wiley & Sons, Ltd.

This article was originally published in the *Encyclopedia of Inorganic Chemistry* in 2006 by John Wiley & Sons, Ltd.
DOI: 10.1002/9781119951438.eibc0264

Of great significance is the synthesis of an extra-large pore microporous material in the aluminophosphate composition. VPI-5, a hydrated aluminophosphate, has a unidimensional channel with a window size formed by 18 tetrahedral cations. At the time of its discovery, the largest window size for zeolites was only 12. Thus, the discovery of VPI-5 inspired new efforts aimed toward the synthesis of extra-large pore microporous materials. Since then, a number of extra-large pore phosphates and silicates have been synthesized. Chalcogenide and metal–organic framework materials offer new promises for the development of extra-large pore materials.

Compared with microporous phosphates, there are few microporous arsenates. The syntheses and structures of arsenates are similar to those of phosphates when divalent metal cations such as Zn^{2+} and Be^{2+} are employed as framework tetrahedral atoms.[12] However, there is very little similarity between alumino- (or gallo-) arsenates and the corresponding phosphates. In the intermediate range where both divalent and trivalent metal cations are present, some similarities between arsenates and phosphates have been observed.[13]

2.3 Microporous Sulfides and Selenides[14,15]

The replacement of framework anions (i.e. O^{2-}) with chalcogens (e.g. S^{2-}) represents a more recent approach for generating microporous materials. The efforts to make microporous chalcogenides began with germanium or tin sulfides. However, germanium or tin sulfides do not form microporous materials similar to all-silica polymorphs of zeolites. It was later found that the incorporation of low-valent cations such as Mn^{2+} into the Ge–S composition helped to generate 3D frameworks.

Three-dimensional sulfide and selenide frameworks have also been made in the indium and gallium chalcogenide compositions. In addition, the incorporation of mono or divalent cations into indium or gallium chalcogenide compositions has produced some new framework chalcogenides often based on the assembly of chalcogenide clusters.

The combination of trivalent (M^{3+}) and tetravalent (M^{4+}) cations in chalcogenides has led to a series of framework chalcogenides, among which the microporous behavior has been demonstrated. The M^{4+} to M^{3+} ratio in these chalcogenides, however, can be much smaller than that in zeolites and so far falls within the range from about 0.21 to 0. Despite the low M^{4+} to M^{3+} ratio, some sulfides in this series possess adequate stability toward ion exchange and thermal treatment. The Cs^{+} exchanged UCR-20GaGeS-TAEA (TAEA = tris(2-aminoethyl)amine) exhibits the type-I isotherm and its pore size is as large as 9.5 Å.[16]

Similar to zeolites, chalcogenides could be prepared with either inorganic or organic cations as extra-framework species. A family of hydrated sulfides and selenides were made recently. These materials, denoted as ICF-*m*, were prepared in aqueous solutions from simple inorganic salts. One of the most interesting properties of these inorganic chalcogenides is fast-ion conductivity at room temperature and moderate to high humidity. In particular, lithium compounds such as ICF-22 and ICF-26 exhibit ionic conductivity significantly greater than previously known crystalline lithium compounds.[6]

2.4 Inorganic–Organic Hybrid Microporous Materials[17]

A rapidly developing field in the microporous materials involves metal–organic framework materials. These materials are prepared by using multidentate organic ligands (e.g. nitriles, carboxylates, amines) to link together metal cations with a low valence (usually divalent cations such as Zn^{2+}). The resulting materials are now called metal–organic frameworks or MOFs.

One promising application of metal–organic frameworks is in the area of gas storage. Several metal–organic framework materials have been found to have a high capacity for methane or hydrogen storage. Through proper design of organic ligands and their assembly with metal centers, noncentrosymmetric or chiral frameworks can be prepared. Moreover, because MOFs generally involve transition metal cations, they open up new opportunities in the design of magnetic microporous materials.

3 MESOPOROUS MATERIALS[18,19]

3.1 Synthesis Pathways and Formation Mechanisms[20,21]

3.1.1 Base Synthesis

The synthesis of ordered mesoporous materials in the past decade greatly expanded the range of ordered porous materials and opened up many new opportunities in the design and applications of materials. Of particular importance is the synthetic methodology that is used for the preparation of these materials. Prior to this, the synthesis of porous materials generally involved the use of individual molecules or hydrated clusters of simple ions. In the synthesis of ordered mesoporous materials, however, it is the assembly of surfactant molecules that directs the condensation of inorganic precursors.

Inspired by the similarity between M41S and surfactant/water liquid crystal phases, Mobil scientists proposed two general pathways (Figure 2).[20,21] The first model suggests that the water-surfactant liquid crystal phase serves as the structure-directing element. This model could not explain observations that surfactant-silicate mesophases could form at surfactant concentration as low as 1%, which is too low to form a liquid crystal phase. The second model suggests that the presence of the silicate somehow mediates the ordering of surfactant micelles into the hexagonal (or cubic Ia3d) arrangement. This model was later further developed by Monnier *et al*. into a more general cooperative assembly mechanism.

Encyclopedia of Inorganic and Bioinorganic Chemistry, Online © 2011 John Wiley & Sons, Ltd.

This article was originally published in the *Encyclopedia of Inorganic Chemistry* in 2006 by John Wiley & Sons, Ltd.
DOI: 10.1002/9781119951438.eibc0264

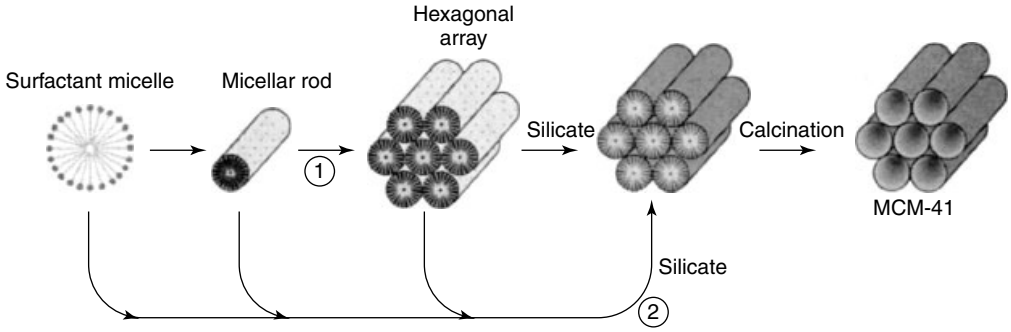

Figure 2 The proposed two possible pathways, (1) and (2), to the formation of MCM-41. (Reprinted with permission from Ref. 21. © 1992 American Chemical Society)

The model by Monnier *et al*. presented a more detailed mechanism by which silicate species can prompt the formation of inorganic–organic composite mesophases.[22] This mechanism suggests that the direct cooperative multidentate binding between cationic surfactants and negatively charged silicate oligomers, preferential polymerization of silicates at the interface, and charge-density matching across the silicate-surfactant interface are crucial factors for the formation of mesophases.

3.1.2 Acid Synthesis

The direct interaction between surfactants and inorganic precursors was later found to be not the only pathway for the formation of mesophases. A major discovery following Mobil's work is the synthesis of mesophases through the assembly of cationic inorganic species with cationic surfactants in acidic solutions. Here, the interaction between cationic silica species and cationic surfactant headgroups is suggested to be mediated by halide anions.

The synthetic results under both basic and acidic conditions allowed Huo *et al*. to propose a generalized mechanism[23,24] for the formation of mesostructured inorganic/organic composites. This mechanism involves electrostatic interactions between the inorganic precursor I and the surfactant headgroup S (Figure 3). Both direct and mediated modes are possible between charged inorganic precursors (cationic I^+, anionic I^-) and charged surfactant headgroups (cationic S^+, anionic S^-), resulting in four synthetic routes: (S^+I^-), (S^-I^+), ($S^+X^-I^+$), and ($S^-M^+I^-$). The (S^+I^-) and ($S^-M^+I^-$) routes occur when the base conditions are used, whereas the (S^-I^+) and ($S^+X^-I^+$) routes are associated with the acid synthesis. The discovery of the acid synthesis approach and the four proposed pathways has had a profound impact on the later development of mesoporous materials.

Zhao *et al*.[25,26] greatly extended the utility of the acid synthesis approach when they used amphiphilic triblock copolymers to prepare a series of periodically ordered

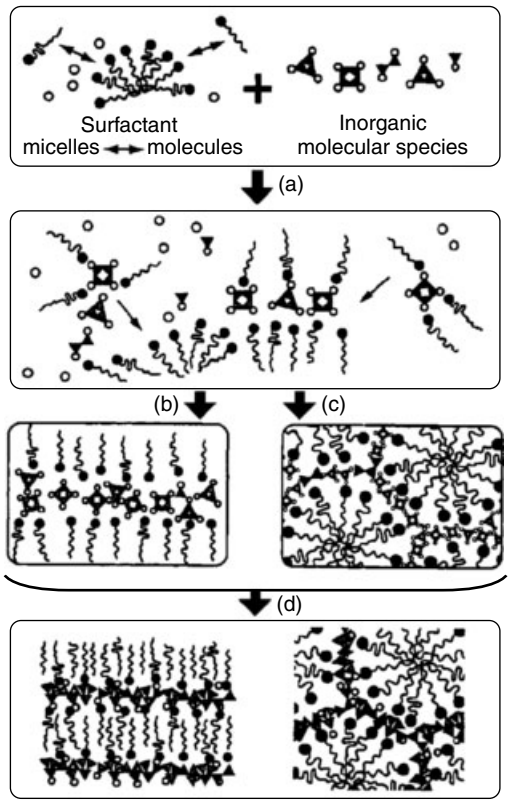

Figure 3 Schematic illustration of interaction between surfactants and inorganic species. (Reprinted with permission from Ref. 24. © 1994 American Chemical Society)

mesoporous silicas, SBA-*n* ($n = 11$, 12, 14, 15, and 16), with uniform pore sizes well beyond 100 Å. Prior to this work, mesoporous materials with pore size in this range either did not exist or had much lower ordering compared to SBA-*n*. The formation of SBA-*n* from block copolymers was proposed to go through the (S^0H^+) (X^-I^+) pathway in the acidic media involving a combination of electrostatic and hydrogen-bonding interactions.[26] The use of the acidic media

Encyclopedia of Inorganic and Bioinorganic Chemistry, Online © 2011 John Wiley & Sons, Ltd.

This article was originally published in the *Encyclopedia of Inorganic Chemistry* in 2006 by John Wiley & Sons, Ltd.
DOI: 10.1002/9781119951438.eibc0264

is a major difference between this work and the earlier work by Pinnavaia *et al*.

In the above work by Zhao *et al*., when the amount of the swelling agent (i.e. 1,3,5-trimethylbenzene) was gradually increased, a structural transition from the hexagonally ordered mesophases into mesostructured cellular foams (MCFs) occurred.[27] The MCFs were made from a system composed of aqueous HCl, triblock copolymer P123, 1,3,5-trimethylbenzene (TMB), and ethanol. Tetraethoxysilane (TEOS) was hydrolyzed at the organic–inorganic interface at the surface of P123-coated TMB droplets in aqueous HCl to form hydrophilic cationic silica species that subsequently condensed around the organic assemblies. The MCFs possess uniform spherical cells with controllable diameter ranging from 24 to 42 nm, depending on the amount of TMB and aging temperature.[28]

3.1.3 Neutral Synthesis

Pinnavaia *et al*.[29] used neutral alkylamines as templates to form disordered mesoporous silica, named hexagonal molecular sieves (HMS). The S^0I^0 formation mechanism was proposed between neutral amine micelles (S^0) and neutral inorganic precursors (I^0). The interactions between S^0 and I^0 were assumed to be hydrogen bonding. The resulting HMS has a 'worm-like' pore structure, with thicker framework walls and smaller X-ray scattering domain sizes compared to M41S.

Mesoporous silica could also be prepared using nonionic amphiphilic surfactants (N^0)[30] with a polyethylene oxide (PEO, EO_n) hydrophilic headgroup. Through the proposed neutral N^0I^0 assembly pathway, worm-like disordered mesoporous silica or amorphous silica are formed using nonionic PEO surfactants or triblock copolymers. The low structural order may be related to the absence of sufficiently strong electrostatic or hydrogen-bonding interactions.

The above N^0I^0 pathway was later modified by Pinnavaia *et al*. by introducing small metal cations ($M^{n+} = Li^+$, Co^{2+}, Ni^{2+}, Mn^{2+}, and Zn^{2+}) into the assembly process, affording mesoporous silica with improved structural order.[31] This approach was denoted $(N^0M^{n+})I^0$, wherein hydrogen bonds were formed between cationic metal complexes containing nonionic $R(EO)_nH$ surfactants (N^0) and the neutral inorganic precursors (I^0). Electrostatic forces were enhanced through the complexation of small M^{n+} cations by the EO groups of N^0. As summarized in Table 1, various types of interactions between the organic surfactants and the inorganic precursors, including electrostatic charge matching (S^+I^-, S^-I^+, $S^+X^-I^+$, and $S^-M^+I^-$), H-bonding (S^0I^0 and N^0I^0), covalent interactions or their combination ((S^0H^+) (X^-I^+) and $(N^0M^{n+})I^0$), may play significant roles in the formation of mesostructured materials.

3.1.4 Ligand-assisted Templating Mechanism

Antonelli and Ying prepared hexagonally packed mesoporous niobium oxide (2D-hexagonal, *p*6m), named Nb-TMS1, using alkyl amines as the structure-direct agent.[32] A new mechanism called 'ligand-assisted templating' (LAT) was suggested. The proposed mechanism involves direct covalent interactions between the Nb alkoxide precursor and the amine ligand through the N–Nb bond prior to the hydrolysis and condensation of the preformed alkoxide-surfactant precursor. After removal of the surfactant by extraction, mesostructures are retained. This approach provides control of mesostructured phases by simple adjustment of the metal/surfactant ratio, resulting in a family of mesoporous transition metal oxides ('$P6_3/mmc$' hexagonal Nb-TMS2, cubic $Pm3n$ Nb-TMS3, and lamellar Nb-TMS4).[33]

3.1.5 Direct Liquid Crystal Templating Mechanism[34]

Mesoporous materials described so far are prepared under surfactant concentrations that are generally too low to form long-range ordered lyotropic liquid crystal phases in a surfactant/water system. The coorganization between inorganic and organic species is prompted by various forms of interfacial interactions, and in general, the stronger the interaction, the more ordered the resulting mesophases.

Mesoporous materials can also be prepared at high surfactant concentrations at which long-range liquid crystals can form even in the absence of inorganic precursors. Attard *et al*. demonstrated this approach by using the liquid crystal phases of the nonionic surfactants such as octaethylene glycol monododecyl ether ($C_{12}EO_8$) or octaethylene glycol monohexadecyl ether ($C_{16}EO_8$) as templates. This synthesis approach is reminiscent of pathway 1 of the original liquid crystal templating mechanism for MCM-41 proposed by Mobil scientists.

In Attard's approach, tetramethylorthosilicate (TMOS) was hydrolyzed and condensed in the aqueous domain of the liquid crystal phase at pH of about 2, leading to mesostructured hexagonal, cubic, or lamellar silica. Methanol from the hydrolysis of TMOS destroys the long-range order of the liquid crystal; however, upon the removal of methanol, the lyotropic liquid crystal is restored and serves as the template phase for the further condensation of silicates. The resulting pore system replicates the shape of the lyotropic mesophase, so this process is also termed 'nanocasting'.

Feng *et al*. prepared a series of periodically ordered mesoporous silica by using high concentrations of triblock copolymers in multicomponent ternary (surfactant/cosurfactant/water) and quaternary (surfactant/cosurfactant/oil/water) systems.[35] One key feature to Feng's approach is that methanol is removed under vacuum prior to the mixing between silicate precursors and surfactants. Thus the lyotropic liquid crystal phase, once formed, maintains its long-range ordering throughout the whole silicate condensation process. The removal of methanol prior to mixing with surfactant/cosurfactant/oil is also advantageous because the presence of surfactant, cosurfactant, or oil could make the

Encyclopedia of Inorganic and Bioinorganic Chemistry, Online © 2011 John Wiley & Sons, Ltd.

This article was originally published in the *Encyclopedia of Inorganic Chemistry* in 2006 by John Wiley & Sons, Ltd.
DOI: 10.1002/9781119951438.eibc0264

Table 1 The general scheme of the various types of interaction between surfactants and inorganic precursors

Pathway[a]	Interaction	Schematic representation	pH	Typical examples of phases formed	Reference
S^+I^-	electrostatic	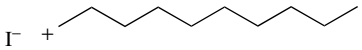	11 – 13	MCM-41, hexagonal MCM-48, cubic MCM-50, lamellar	Mobil, 1992[20,21]
S^-I^+	electrostatic	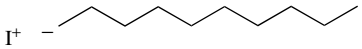	<5	Metal Oxides, lamellar	Stucky, 1994[23,24]
$S^+X^-I^+$	electrostatic	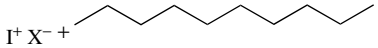	<2	Silica, hexagonal, cubic, lamellar	Stucky, 1994[23,24]
$S^-M^+I^-$	electrostatic	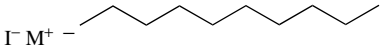	>8	ZnO, Al_2O_3, lamellar	Stucky, 1994[23,24]
S^0I^0	H-bonding	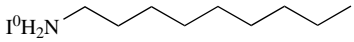	~9	HMS, worm-like	Pinnavaia, 1995[29]
N^0I^0	H-bonding	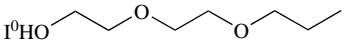	≤7	MSU family, worm-like	Pinnavaia, 1995[30]
LAT (S-I)	Covalent	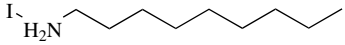		Nb-TMS, M41S analogs	Ying, 1996[32]
$(S^0H^+)(X^-I^+)$	Electrostatic + H-bonding	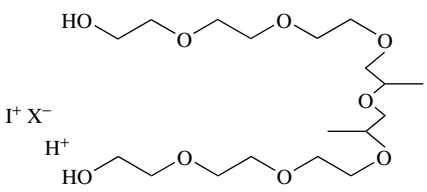	<1	SBA-15, hexagonal	Stucky, 1998[25,26]
$(N^0M^{n+})I^0$	Electrostatic + H-bonding	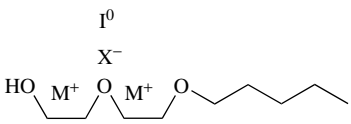	~7	Hexagonal or 3D faulted hexagonal and cubic	Pinnavaia, 1999[31]

[a] S = surfactants; I = inorganic species; M^{n+} = metal cations; X^- = halide anions; N = nonionic surfactants.

efficient removal of methanol difficult. The use of cosurfactants and oils provides additional variables for the control of a number of structural features of resulting mesophases including pore size and wall thickness.

During the direct liquid crystal templating, the condensation of inorganic precursors occurs in the aqueous domain of preformed lyotropic liquid crystals. With this approach, the interaction between inorganic precursors and surfactant headgroups could disrupt the long-range order of liquid crystals and should therefore be minimized. For silicates, performing reactions at pH of about 2, which is the isoelectric point of silicates, helps to reduce such interaction.

3.1.6 Evaporation-induced Self-assembly (EISA)

Brinker *et al*. developed a simple evaporation-induced self-assembly (EISA) process that allows the rapid production of patterned porous or nanocomposite materials in the form of films, fibers, or spheres.[36] Starting from a homogeneous solution of soluble silica and surfactant below the critical micellar concentration, evaporation of ethanol increased surfactant concentration, driving self-assembly of silica-surfactant micelles and their further organization. By adjusting the initial alcohol/water/surfactant molar ratio, 2D hexagonal, cubic, 3D hexagonal, and lamellar silica-surfactant mesophases could be made.

3.2 Structure[37]

The pore structure, such as pore geometry and pore size, of mesoporous materials is one of the key parameters for practical applications, especially those dependent on size and shape selectivity and ready access to porosity. Considerable efforts have been devoted to control the pore structure of mesoporous materials.

3.2.1 Pore Geometry Control

The pore geometry is associated with the symmetry of mesophases and can be ill defined when the ordering of the mesophases is very low. However, highly ordered mesophases can be prepared under a variety of experimental conditions. By tuning synthetic parameters, it is possible to control the topological features of resulting mesophases. The original Mobil work led to the synthesis of a 2D ordered hexagonal

Encyclopedia of Inorganic and Bioinorganic Chemistry, Online © 2011 John Wiley & Sons, Ltd.

This article was originally published in the *Encyclopedia of Inorganic Chemistry* in 2006 by John Wiley & Sons, Ltd.
DOI: 10.1002/9781119951438.eibc0264

phase with unidimensional channels ($p6m$) and a 3D ordered cubic phase with 3D bicontinuous channels (Ia3d). The use of the acidic medium and the surfactant $C_{16}H_{33}N(C_2H_5)_3^+$ or $C_{16}H_{33}N(C_2H_5)(C_5H_{10})^+$ (cetylethylpiperidinium) allowed Huo *et al*. to discover a new cubic phase (Pm3n), SBA-1.[24] In addition, SBA-2[38] (acid synthesis) and SBA-7[39] (base synthesis) with previously unknown pore structure were also prepared by using divalent quaternary ammonium surfactants with the general formula $C_nH_{2n+1}N(CH_3)_2(CH_2)_sN(CH_3)_3^{2+}$ (denoted C_{n-s-1}, $n = 12, 13, 16, 18, 20$, $s = 2, 3, 6$). Two new cubic mesoporous silica SBA-11 (*Pm*-3*m*) and SBA-16 (*Im*-3*m*) have been synthesized by Zhao *et al*. from $C_{16}EO_{10}$ and $EO_{106}PO_{70}EO_{106}$,[26] respectively, in addition to SBA-12 that is similar in structure to SBA-2.

The use of surfactant molecules with different charges and geometrical features is an effective way to control the structure of mesophases. According to the cooperative self-assembly formation mechanism, inorganic species interact with surfactant micelles at the interface through electrostatic interaction or hydrogen bonding. So phase transitions are expected to be associated with changes in the curvature of interface. In classical micelle chemistry, micellar organization is related to the local effective surfactant packing parameter, $g = V/a_0l$, where V is the total volume of the hydrophobic chains, a_0 is the effective headgroup area at the micelle surface, and l is the kinetic surfactant tail length. The expected mesophase depends on the value of g (Table 2). Huo *et al*. first applied this concept to explain and predict product structure and phase transition.[38,40]

Other factors that affect the structure of mesophases include the concentration ratio between surfactants and inorganic precursors. For example, MCM-41 was prepared at a $C_{16}H_{33}(CH_3)_3N^+$/Si ratio of less than 1. As the $C_{16}H_{33}(CH_3)_3N^+$ /Si ratio increases beyond 1, the cubic phase (Ia3d) can be produced. Similarly, Nb-TMS1 ($p6m$), Nb-TMS2 ($P6_3/mmc$), Nb-TMS3 (Pm-3n), and Nb-TMS4 ($p2$) were prepared at various surfactant to Nb ratios.[33]

3.2.2 Pore Size Engineering

Surfactant Chain Length. Under comparable reaction conditions, the pore size generally increases with the chain length of surfactants. For example, when quaternary ammonium surfactants (C_nTMABr) with different alkyl tails ($n = 8$, 9, 10, 12, 14, and 16) were used, the pore size of resulting materials increased from 18 to 37 Å with the increase in the chain length.[21]

Table 2 Different g values and related mesophases

g	Mesophase	Space group	Examples
$<1/3$	3D hexagonal	$P6_3/mmc$	SBA-2
1/3	Cubic	$Pm3n$	SBA-1
1/3 – 1/2	2D hexagonal	$p6m$	SBA-3, MCM-41
1/2 – 2/3	Cubic	$Ia3d$	MCM-48
>1	Lamellar	$p2$	MCM-50

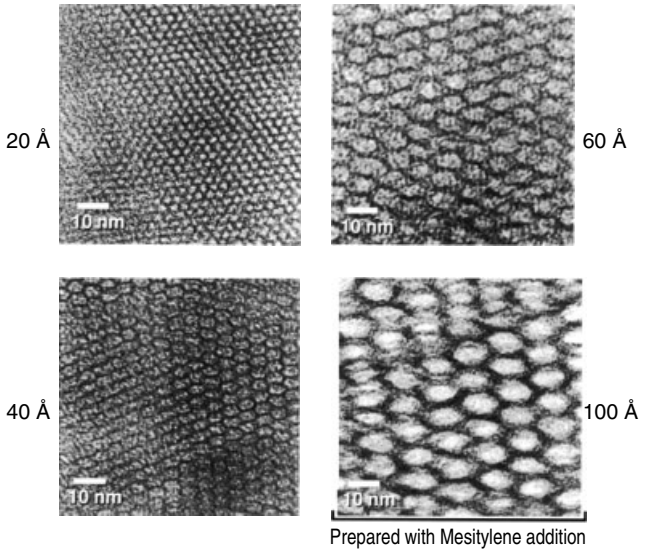

Figure 4 TEM images of MCM-41 with different pore sizes up to 100 Å. (Reprinted with permission from Ref. 21. © 1992 American Chemical Society)

Addition of Swelling Agents. In Mobil's original work on M41S, 1,3,5-TMB was used as the swelling agent to increase the pore size of mesoporous materials. By adjusting the TMB/C_{16}TMABr ratios, the pore size of MCM-41 was enhanced up to 100 Å (Figure 4). Other aromatic hydrocarbons, alkanes, and amines have also been used as pore expanders. Owing to their hydrophobicity, organic auxiliaries can be incorporated into the core of micelles to increase the size of micelles. The increase in the pore size of resulting mesophases is related to this phenomenon.

Temperature[41]. The N^0I^0 synthetic pathway can be used to control the pore size by choice of the assembly temperature. In the case of MSU-1 silica assembled with Tergitol 15-S-12, pore size increases from 21 to 45 Å when the synthesis temperature is increased from 25 to 65 °C. With increasing temperature, PEO segments of the surfactant become more hydrophobic, thus decreasing the size of hydrophilic headgroups and, consequently, enlarging the diameter of hydrophobic core, which determines the pore size. The hydrogen bonding between the shortened hydrophilic PEO segments of surfactants and inorganic species, which is related to the wall thickness, can become weaker at elevated temperatures. This mechanism is supported by the evidence of a decrease in the wall thickness accompanied by an increase in the pore size.

Encyclopedia of Inorganic and Bioinorganic Chemistry, Online © 2011 John Wiley & Sons, Ltd.

This article was originally published in the *Encyclopedia of Inorganic Chemistry* in 2006 by John Wiley & Sons, Ltd.
DOI: 10.1002/9781119951438.eibc0264

Postsynthesis Treatment[42]. As-synthesized mesoporous silica can contain a significant concentration of the OH^- group, particularly if made at low synthesis temperatures and in short times, and their pore size can be modified by the postsynthesis treatment. Tailoring the pore size through this method is commonly achieved by hydrothermal restructuring of as-synthesized materials at a higher temperature. A gradual pore size expansion to about 70 Å was observed by treatment of as-made MCM-41 in the mother liquid at 150 °C for a period of 1 to 10 days.[43] Huo and coworkers found that the pore size of MCM-41 could be enlarged by hydrothermal treatment of the predried, as-made samples at 100 °C, affording high-quality materials with the pore size up to 60 Å.[24]

Water is thought to enter the pore space to solvate the silicate framework, surfactants, and their counterions, leading to silica dissolution, transport, and redeposition. It is shown that the hydrothermal restructuring process is very sensitive to both the temperature and the duration. While an excessive hydrothermal treatment can cause dramatic decreases of pore volumes and surface areas, neutral amines and alkenes generated in situ by the decomposition of some quaternary ammonium surfactants can act as swelling agents. The water-amine postsynthesis treatment provides further support for the swelling effect of neutral amines. Sayari *et al*. reported pore size expansion by up to threefold when as-synthesized MCM-41 was treated in aqueous emulsions of an appropriate long-chain amine, such as *N*,*N*-dimethylhexadecylamine (DMHA).[44] An unprecedented enlargement of pore size (from 31.5 to 250 Å) and pore volume (from 0.85 to 3.31 $cm^3\ g^{-1}$) was achieved by hydrothermal treatment in the presence of dimethyldecylamine (DMDA).[45]

3.3 Composition

3.3.1 Silica and Doped Silica

A large variety of mesoporous silica has been prepared. These mesoporous silicas differ in a number of features including space group symmetry, degree of ordering, pore size and wall thickness, and degree of polymerization. As shown in Table 3, these differences are generated by a number of synthetic factors such as pH, types of surfactants, and auxiliary reagents such as oils and inorganic ions. Many different names exist for mesoporous silica, and these different names designate materials prepared under specific conditions used by different individual research groups.[46–52]

Numerous efforts have been spent on doping silica with other elements, most of which are transition metal elements. In many cases, the goal of these syntheses is to introduce or enhance acidic or redox catalytic activity into mesoporous silica. Depending on the individual element and synthetic procedures, the doping level spans a wide range of values from about 5 to over 3000 for the Si/dopant molar ratio.[54]

3.3.2 Phosphates

Because of the similarity between aluminophosphate and silica molecular sieves, the synthesis of mesoporous silica was soon followed by the efforts aimed toward the synthesis of mesoporous aluminophosphates. Both lamella and hexagonally ordered aluminophosphate mesostructures have been prepared.[55,56]

Recently, Zhao *et al*. proposed that the interaction between two or more inorganic precursors, guided by 'acid–base pair' principles, plays an important role in the formation of ordered multicomponent mesoporous structures, in particular phosphates.[57] They suggested that to form multicomponent mesoporous materials, stable pairs of different species during nucleation are necessary. The larger the acidity or alkalinity difference between the metallic and nonmetallic precursors, the more likely that the pairs will form. No extra acid or base is required to adjust the pH of the synthesis system. This method is particularly effective for metal phosphates. A series of mesoporous materials including TiPO, ZrPO, AlPO, NbPO, and CePO were prepared by using this approach.

3.3.3 Metal Oxides

Mesoporous metal oxides encompass a variety of chemical compositions. In general, these compositions are not as stable as mesoporous silica, or they are not as ordered as silica. However, the combination of mesoporosity with other unique properties afforded by these compositions (e.g. semiconductivity, redox activity) has inspired considerable efforts in the synthesis of these mesostructured materials. In the study of synthetic pathways for the formation of mesoporous materials, Huo *et al*. reported a series of mesostructured oxides based on Sb, W, and Al and so on. by using cationic or anionic surfactants.[24] Another significant progress in the templated synthesis of mesoporous oxides was reported by Yang *et al*. when they used block copolymers to synthesize a range of mesoporous oxides including TiO_2, ZrO_2, HfO_2, Nb_2O_5, Ta_2O_5, WO_3, Al_2O_3, SiO_2, and SnO_2.[58] Yang's approach is also applicable to the synthesis of mixed oxides such as Al_2TiO_y and $ZrTiO_y$. The following gives a discussion of some selected mesoporous oxides.

Titania. Mesoporous TiO_2 is very attractive because of the excellent photocatalytic activity associated with TiO_2. Among the three crystalline polymorphs of titania (anatase, rutile, and brookite), anatase is the most suitable phase for photocatalysis because of its large band gap and suitable redox potential. The early attempts to prepare mesoporous titania used surfactants with phosphate headgroups, and the resulting mesophases contain phosphate groups even after calcinations.[59,60] Phosphorus-free mesoporous titania was reported by Antonelli by using dodecylamine.[61] Using block copolymers, Yang *et al*. reported the synthesis of

Encyclopedia of Inorganic and Bioinorganic Chemistry, Online © 2011 John Wiley & Sons, Ltd.

This article was originally published in the *Encyclopedia of Inorganic Chemistry* in 2006 by John Wiley & Sons, Ltd.
DOI: 10.1002/9781119951438.eibc0264

Table 3 A summary of various silicate mesophases

Name	Mesophase	Space group	Surfactant	Pathway
MCM-41[20,21]	Hexagonal	*p6m*	alkylammonium, e.g. CTAB	S^+I^-
MCM-48[20,21]	Cubic	*Ia3d*	alkylammonium, e.g. CTAB	S^+I^-
MCM-50[20,21]	Lamellar	*p2*	alkylammonium, e.g. CTAB	S^+I^-
MSU-1[30]	Wormhole/disordered		Tergitol, e.g. $C_{11-15}EO_9$	S^0I^0
MSU-2[30]	Wormhole/disordered		Triton-X, e.g. C_8PhEO_8	S^0I^0
MSU-3[30]	Wormhole/disordered		Pluronic, e.g. $EO_{13}PO_{30}EO_{13}$	S^0I^0
MSU-4[30]	Wormhole/disordered		Tween	S^0I^0
MSU-G[46]	3D vesicular	L_3	gemini diamines, e.g. $C_{10}H_{21}NH(CH_2)_2NH_2$	N^0I^0
HMS[29]	Wormhole/disordered		amines, e.g. C_8NH_2	N^0I^0
SBA-1[24]	Cubic	*Pm-3n*[51]	alkylammonium	$S^+X^-I^+$
SBA-2[38]	3D hexagonal	$P6_3/mmc$	divalent quaternary ammonium	S^+I^-
SBA-3[20]	hexagonal	*p6m*	quaternary ammonium (acid synthesis)	$S^+X^-I^+$
SBA-4[39]	lamellar	*P2*		base
SBA-5[39]	cubic	*R3c*		base
SBA-6[39]	cubic	*Pm-3n*[51]	$18B_{4-3-1}$ gemini[a]	base
SBA-7[39]	3D hexagonal	$P6_3/mmc$		$S^+X^-I^+$
SBA-8[53]	2D rectangular	*cmm*	cationic bolaform[b]	S^+I^-
SBA-11[26]	cubic	*Pm3m*	alkyl-polyethylene oxide, e.g. $C_{16}EO_{10}$	$(S^0H^+)(X^-I^+)$
SBA-12[26]	3D hexagonal	$P6_3/mmc$	alkyl-polyethylene oxide, e.g. $C_{18}EO_{10}$	$(S^0H^+)(X^-I^+)$
SBA-14[26]	cubic	*Pm3n*	alkyl-polyethylene oxide, e.g. $C_{12}EO_4$	$(S^0H^+)(X^-I^+)$
SBA-15[25,26]	2D hexagonal	*p6m*	block copolymer, e.g. $EO_{20}PO_{70}EO_{20}$	$(S^0H^+)(X^-I^+)$
SBA-16[26]	cubic	*Im-3m*[51]	block copolymer, e.g. $EO_{106}PO_{70}EO_{106}$	$(S^0H^+)(X^-I^+)$
FDU-1[47]	cubic, caged	*Fm3m*[52]	$EO_{39}BO_{47}EO_{39}$	(S^0H^+) (X^-I^+)
KIT-1[48]	disordered		$[C_{16}H_{33}N(CH_3)_3]^+Cl^-$	S^+I^-
FSM-16[49]	layered		$[C_{16}H_{33}N(CH_3)_3]^+Cl^-$	sheets folding
PCH[50]	layered		intercalated quaternary ammonium and neutral amine	gallery-templated

[a]Gemini surfactant 18B4-3-1 = $C_{18}H_{37}OC_6H_4OC_4H_8N(CH_3)_2C_3H_6N(CH_3)_3Br_2$. [b]Bolaform surfactant $(CH_3)N–(CH_2)_n–O–(C_6H_4)_2–O–(CH_2)_n–N(CH_3)_3Br_2$, $n = 4, 6, 8, 10, 12$.

2D hexagonal titania from $EO_{20}PO_{70}EO_{20}$ and cubic titania (*Im3m*) from $EO_{75}BO_{45}$.[58]

Very recently, mesoporous TiO_2 with anatase, rutile, bicrystalline mixture (anatase and rutile) with controlled phase composition, and tricrystalline mixture (anatase, rutile, and brookite) were reported by using triblock copolymer as template and $TiCl_4$ as precursor.[62] The resulting crystalline titanias are thermally stable and have high surface area and large pore size up to 16 nm.

Zirconia. Mesoporous zirconia was first reported by Knowles and Hudson[63] with cationic alkyltrimethylammonium surfactants.[64] Starting from zirconium sulfate or propoxide, Schüth[65] and Ciesla *et al*.[66] synthesized hexagonal mesoporous zirconia using alkyltrimethylammonium surfactants as templates. Reddy and Sayari[67] obtained hexagonal or lamellar phases of mesostructured zirconia using quaternary ammonium surfactants and acidified primary alkylamine, respectively. Mesoporous zirconia has also been synthesized with amphoteric[68] and anionic[69,70] templates.

In a detailed study,[71] mesostructured zirconia has been prepared by using various amphiphilic surfactants with different headgroups (anionic and nonionic) and different tail lengths (1–18 carbons) as templates. Removal of surfactants leads to the loss of structural order and a decrease of the surface area. However, the presence of phosphates and sulfates in the walls may improve the stability.

Alumina. Mesoporous aluminas with high surface area are of great interest because of their potential use as catalysts and catalyst supports. The first successful synthesis of mesoporous aluminas was reported by Bagshaw and Pinnavaia through N^0I^0 assembly process.[72] Aluminas accessible through this route (designated as MSU-X aluminas) have wormhole pore structures with surface area around 400 to

Encyclopedia of Inorganic and Bioinorganic Chemistry, Online © 2011 John Wiley & Sons, Ltd.

This article was originally published in the *Encyclopedia of Inorganic Chemistry* in 2006 by John Wiley & Sons, Ltd.
DOI: 10.1002/9781119951438.eibc0264

500 $m^2\ g^{-1}$. Similar wormhole mesoporous aluminas were also prepared using cationic[73] or anionic[74] surfactants as templates.

Mesostructured alumina with hexagonal structure can be synthesized in the presence of sodium dodecyl sulfate (SDS), but it was not stable upon surfactant removal.[75] Thermally stable mesoporous alumina has been obtained by using triblock copolymer as templates in ethanol solution. Most alumina mesophases consist of amorphous or semicrystalline framework. Recently, Pinnavaia and coworkers developed a novel three-step assembly method to prepare mesostructured alumina with framework walls composed of crystalline, lathlike γ-Al_2O_3 nanoparticles.[76,77]

3.3.4 Carbons[78]

Porous carbonaceous materials are important in many application areas because of their remarkable properties, such as high surface areas, chemical inertness, and good mechanical stability. Carbon molecular sieves that are amorphous and microporous are commercially important for the separation of nitrogen from air, and activated carbons with a wide pore size distribution are also useful adsorbents for various applications.

Recently, there has been an increasing interest in the synthesis of ordered mesoporous carbons,[79] since such materials are very promising as adsorbents, catalyst supports, and electrochemical double-layer capacitors.[80,81] Ordered mesoporous silicas have been shown as suitable templates to prepare periodic mesoporous carbons with various pore shapes and connectivity. The synthesis procedure involves impregnation of the mesoporous silica with an appropriate carbon precursor, carbonization of carbon source, and subsequent removal of silica using an aqueous solution of HF or NaOH.[78]

Ryoo *et al*. reported the first ordered mesoporous carbon, CMK-1, using cubic MCM-48 as template and sucrose as carbon source.[79] CMK-1 exhibited a highly ordered cubic structure, as confirmed by transmission electron microscopy (TEM). However, x-ray powder diffraction patterns indicated that CMK-1 underwent a structural transformation upon the silica removal due to the two disconnected porous systems separated by the silica wall.[82,83]

Similarly, cubic SBA-1 and disordered HMS have also been used as templates to prepare periodic mesoporous carbons (designated as CMK-2[79] and SNU-2[84] respectively). On the other hand, MCM-41 that has a hexagonal structure with unidimensional channels was found unsuitable as the template for the preparation of mesoporous carbons. Using SBA-15 as a template resulted in the first-ordered mesoporous carbon, designated as CMK-3,[85] which is exactly an inverse replica of the silica template. Although SBA-15 possesses the hexagonal mesostructure (p6m) similar to MCM-41, the microporosity[86] or the mesotunnels[87] within the silica walls could be responsible for the successful replication of ordered CMK-3.[88] Recent work on periodic mesoporous carbons includes improving structural integrity and thermal stability,[89] developing a low-cost synthesis route,[90] controlling the pore diameters,[91] and preparing carbons with graphitic pore walls.[92]

3.3.5 Periodic Mesoporous Organosilicas (PMOs)

Periodic mesoporous organosilicas (PMOs) are a new kind of organic–inorganic hybrid materials. However, unlike hybrid mesoporous materials made by grafting organic groups on the pore surface, PMOs contain organic groups as an integral component of silica-based framework.[93–95] The synthesis of PMOs involves the hydrolysis and condensation of tailor-made bridged organosilica precursor $((R'O)_3Si)_nR$ ($n = 2$ or 3, $R' =$ methyl or ethyl) in the presence of surfactant assemblies. The surfactant templates can be removed by solvent extraction or ion exchange. Essential to the synthesis of PMOs is the design and selection of the organosilica precursors. Various synthetic routes, such as Grignard, alcoholysis, hydrosilation, Pd-catalyzed Heck coupling, hydroboration, lithiation, and silylation of halides have been applied to prepare the molecular poly(trialkoxysilyl)organic precursors.[96] So far, various organic groups (Figure 5) including methane, ethane, ethylene, and benzene have been integrated into the framework of PMOs.[96,97] Since the first three contributions to PMOs were reported in 1999, some new synthetic strategies have been developed for the preparation of PMOs, resulting in many mesophases including wormhole structures,[95] cubic structures,[98] 2D hexagonal structures similar to MCM-41[93] or SBA-15,[99] and a 3D hexagonal structure with unknown space group.[94] One of the most intriguing successes is the report of a 2D hexagonal mesoporous benzene-silica with a crystal-like wall structure, exhibiting structural periodicity with a spacing of 7.6 Å along the channel direction.[100]

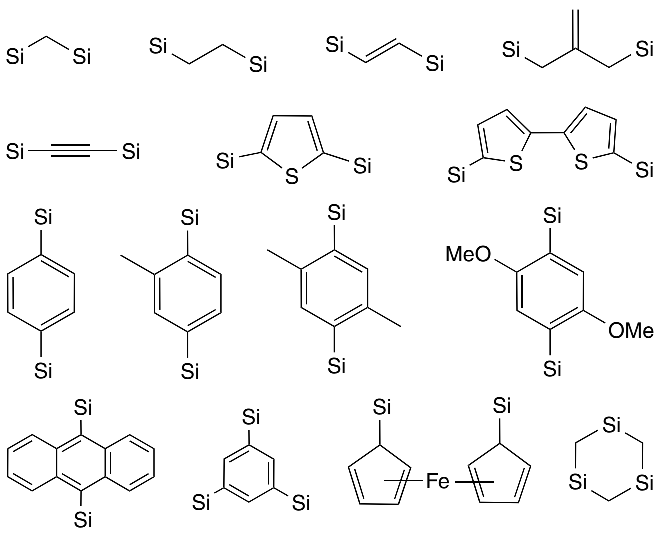

Figure 5 Examples of organic and organometallic bridging groups that have been incorporated into PMOs

Encyclopedia of Inorganic and Bioinorganic Chemistry, Online © 2011 John Wiley & Sons, Ltd.
This article is © 2006 John Wiley & Sons, Ltd.
This article was originally published in the *Encyclopedia of Inorganic Chemistry* in 2006 by John Wiley & Sons, Ltd.
DOI: 10.1002/9781119951438.eibc0264

Advantages[101] of PMOs include homogeneous distribution of bridged organic groups with high and tunable concentrations, large free void space, and consequently easily accessible functional groups. PMOs are expected to provide interesting electronic, optical, magnetic, catalytic, and mechanical properties.[96,101,102]

3.3.6 Chalcogenides

Germanium Sulfides. Metal chalcogenides are among the earliest nonoxide mesostructured materials being studied.[15] Because of the similarity to silicates, germanium or tin chalcogenides have received considerable attention. Through the room temperature reaction of aqueous solutions of $Na_4Ge_4S_{10}$ with solutions of various surfactant alkyltrimethylammonium bromide salts, Kanatzidis *et al*. prepared several surfactant-inorganic phases with the general formula of $[C_nH_{2n+1}N(CH_3)_3]_4Ge_4S_{10}$ ($n = 12$, 14, 16, and 18).[103] All four phases contain unconnected $[Ge_4S_{10}]^{4-}$ clusters and are fully crystalline with the space group P−1, unlike a typical amorphous mesoporous solid.

Ozin *et al*. subsequently prepared hexagonal mesostructured germanium sulfides by using low-valent metal cations such as Co^{2+}, Ni^{2+}, Cu^{+}, and Zn^{2+} to connect $[Ge_4S_{10}]^{4-}$ clusters around cetyltrimethylammonium bromide (CTAB).[104] This approach is similar to the synthesis of microstructured $[(CH_3)_4N]_4Mn[Ge_4S_{10}]$. However, Ozin's approach used formamide as the solvent instead of water.

Mesostructured germanium sulfides containing wormhole-like pores were prepared by Kanatzidis *et al*. by using divalent metal cations such as Zn^{2+}, Cd^{2+}, Hg^{2+}, Ni^{2+}, and Co^{2+} in aqueous medium with cationic surfactants $[C_nH_{2n+1}N(CH_3)_3]Br$ ($n = 12$, 14, 16, and 18). A hexagonally ordered mesostructured manganese germanium sulfide was prepared under hydrothermal conditions with Mn^{2+} as the linking agent and mesityltrimethylammonium surfactant.[105] New hexagonally ordered mesophases could also be made by using Pt^{2+} as the linker in the presence of alkylpyridinium surfactants $[C_nH_{2n+1}NC_5H_5]Br$ ($n = 12$, 14, 16, 18, 20, and 22).[106]

In addition to divalent metal cations, trivalent and tetravalent cations (i.e. In^{3+}, Ga^{3+}, Sb^{3+}, and Sn^{4+}) were also effective as linking agents to organize $[Ge_4S_{10}]^{4-}$ clusters to form hexagonally ordered mesostructures.[107,108] In this case, cetylpyridinium bromide was used as the surfactant, and formamide served as the solvent. The mesophases made with Ga^{3+} and Sb^{3+} showed intense visible photoluminescence at 77 K.

In all the above cases, metal cations are used as linking agents to connect together $[Ge_4S_{10}]^{4-}$ clusters. It can be envisioned that it might also be possible to employ metal clusters to link $[Ge_4S_{10}]^{4-}$. One such cluster is the biologically relevant cubane Fe_4S_4. Starting from $K_4Ge_4S_{10}$ and substitutionally labile $[Fe_4S_4Cl_4]^{2-}$ clusters, a novel hexagonally ordered mesostructured sulfide built from both $[Ge_4S_{10}]^{4-}$ and $[Fe_4S_4Cl_4]^{2-}$ clusters was synthesized from a formamide solution containing the surfactant cetylpyridinium bromide.[109]

Tin Sulfides. Kessler *et al*. reported a crystalline phase synthesized from $SnCl_4$, Na_2S, and dodecylamine in the ethanol-water system at room temperature. This new tin sulfide has the formula of $(C_{12}H_{25}NH_3)_4[Sn_2S_6]{\cdot}2H_2O$, and the $[Sn_2S_6]^{4-}$ dimers are formed by two edge-sharing $[SnS_4]$ tetrahedra.[110] Hexagonally ordered mesostructured tin sulfides were synthesized by Kanatzidis *et al*. by linking $[Sn_2S_6]^{4-}$ clusters with metal cations (i.e. Zn^{2+}, Cd^{2+}, Ga^{3+}). These photoluminescent mesophases were made in the presence of cetylpyridinium surfactant in the formamide solution under basic conditions and are semiconductors in the energy range from 2.5 to 3.1 eV.[111]

Germanium Selenides. Mesostructured germanium selenides are chemically and structurally similar to the corresponding sulfides. By following strategies similar to those developed for sulfides, Kanatzidis *et al*. have prepared a series of mesostructured germanium selenides. By using Zn^{2+}, Cd^{2+}, Hg^{2+}, Ni^{2+}, and Co^{2+} to link $[Ge_4Se_{10}]^{4-}$ clusters, mesostructured germanium selenides with wormholes were prepared in the presence of cationic surfactants $[C_nH_{2n+1}N(CH_3)_3]Br$ ($n = 12$, 14, 16, and 18).[112] Hexagonally mesostructured selenides were prepared by linking $[Ge_4Se_{10}]^{4-}$ clusters with Pt^{2+}, Sb^{3+}, Sn^{4+} or Fe_4S_4 clusters as linker agents and cetylpyridinium as the surfactant.

Tin Selenides. A series of mesostructured tin selenides were prepared by Kanatzidis *et al*. by linking $[SnSe_4]^{4-}$ anions with divalent metal cations.[113] These materials have the general formula of $(CP)_{4-2x}M_xSnSe_4$, where CP is cetylpyridinium; $1.0 < x < 1.3$; M = Mn, Fe, Co, Zn, Cd, and Hg. The *d*-spacing for the lowest peak ranges from 35 to 40 Å, and the pore arrangement based on wormhole, hexagonal, and cubic types has been observed. These phases are medium band gap semiconductors with band gap varying from 1.4 to 2.5 eV.

In addition to $[SnSe_4]^{4-}$ anions, $[Sn_2Se_6]^{4-}$ dimers could also form mesophases in combination with Pt^{2+} in the presence of long-chain pyridinium surfactants (C_nPyBr, $n = 18$, 20).[114] In this case, the cubic symmetry with the space group Ia-3d was preferred. The surfactant molecules could be ion-exchanged reversibly and without loss of the cubic structure and particle morphology. This Pt−Sn−Se phase has a low-energy band gap of 1.7 eV.

Similar to germanium sulfides or selenides, $[Sn_4Se_{10}]^{4-}$ adamantine clusters also exist and have been found to form mesostructured semiconductors with Pt^{2+} when templated by the lyotropic liquid-crystalline phase of alkylpyridinium surfactant $[C_{16}H_{33}NC_5H_5]Br$. This mesophase designated as $C_{16}PyPtSnSe$ has a band gap of 1.5 eV.

Encyclopedia of Inorganic and Bioinorganic Chemistry, Online © 2011 John Wiley & Sons, Ltd.

This article was originally published in the *Encyclopedia of Inorganic Chemistry* in 2006 by John Wiley & Sons, Ltd.
DOI: 10.1002/9781119951438.eibc0264

Other Chalcogenides. In addition to germanium (or tin) sulfides and selenides, mesostructured chalcogenides have also been made in other compositions. For example, Stupp *et al*. prepared hexagonally ordered mesostructured CdS by reacting H_2S with cadmium salts within the ordered environment of the preformed liquid crystal mesophase.[115] The mesophase was formed using oligoethylene oxide oleyl ether ($C_{18}H_{35}(OCH_2CH_2)_{10}OH$) mixed with an equal volume of aqueous 0.1 M Cd^{2+} salt. The symmetry and long-range order of the liquid crystal are preserved during the precipitation of the inorganic–organic mesophase.

3.3.7 Metals

By using preformed lyotropic liquid crystals of nonionic surfactants, Attard and coworkers have prepared mesostructured Pt and Sn.[116–118] This methodology can be applied to other elements such as Se and Te or metal alloys such as Pt–Ru or Pt–Pd.[119–121] The ordered mesostructured metals can be obtained by either chemical or electrochemical reduction of metal salts that are dissolved in the aqueous domain of lyotropic liquid crystals formed from oligoethylene oxide nonionic surfactants. The pore diameter can be tuned by the length of the alkyl chain of the surfactants, and the topology of metallic mesophases can be controlled by the symmetry of lyotropic liquid crystals.

The chemical reduction method generally produces mesostructured metals with granular morphology. The mesostructures of the metals formed by this method are casts of the structures of the liquid crystals used in the syntheses. During this process, the product is formed in the aqueous domain of the preorganized liquid crystals without disrupting the long-range ordering of the liquid crystals.

The electrochemical reduction method can produce mesostructured metals in the form of thin films. By electrodeposition of plating mixtures made from appropriate salts, mesostructured metal films can be produced on the electrode surface with high surface areas and good mechanical and electrochemical stability. The ability to produce ordered mesostructured metal films may lead to new types of electrode materials for applications such as batteries, fuel cells, and sensors.

3.4 Morphology Control

Mesoporous materials were originally synthesized in irregular bulk or powder forms, which could limit their applications in separation, optics, electronics, and so on. Thus, it is highly desirable to produce mesoporous materials with controllable macroscopic forms. So far, mesoporous materials have been synthesized in a variety of forms including thin films, spheres, fibers, monoliths, rods, single crystals, and nanoparticles. The acidic synthetic route ($S^+X^-I^+$) developed by Huo *et al*. appears to be the most appropriate for the morphological control of mesostructures.

3.4.1 Thin Films

The interests in thin films of silica-surfactant mesostructured materials arise from their potential applications in membrane-based separations, sensors, heterogeneous catalysis, and microelectronics.[122] Thin films of mesoporous silicas were first prepared by spin-coating an aqueous mixture of surfactants and prehydrolyzed silica precursors on a substrate followed by drying.[123,124] In addition to the spin-coating method, supported films can also be made by directly growing on substrates[125,126] or by dip-coating.[127,128] The film growth is generally faster by spin- or dip-coating. Free-standing films can be grown at liquid–vapor (e.g. water–air)[129,130] and liquid–liquid (e.g. oil–water) interfaces.[131] In addition to mesostructured silica, thin films of mesostructured titania,[132] zirconia,[133] tin oxide,[134] and organosilica[135] have also been successfully achieved.

3.4.2 Spheres

The use of emulsion biphase chemistry allows the preparation of both hollow[136] and hard[137] mesoporous silica spheres. Through a modified Stöber method,[138] spherical mesoporous silicas with particle sizes ranging from submicrometers to micrometers (~2 μm) have been achieved.[139,140] Recent efforts have focused on control of the size and monodispersity. Ward and coworkers have achieved highly monodisperse mesoporous silica spheres with controllable particle size by EISA of precursor microdroplets produced by a vibrating orifice aerosol generator (VOAG).[141] Pseudomorphic transformation of preformed amorphous silica spheres to MCM-41 has demonstrated another promising way for the control of the size and morphology.[142]

3.4.3 Monoliths

There is an increasing interest in transparent monoliths with periodic mesoporous structures due to their potential applications in optics. Using the direct liquid crystal templating approach, Feng *et al*. prepared monolithic mesostructured silica templated by microemulsion liquid crystals.[143] By adjusting the synthetic composition, many different highly ordered mesophases, such as cubic spherical micellar *Im*3*m*, 3D hexagonal $P6_3/mmc$, bicontinuous cubic *Ia*3*d*, and primitive-centered cubic *Pn*3*m*, were obtained.[144] Careful control of evaporation of the solvent by a thin layer of mineral oil also helped the preparation of crack-free monoliths.[145]

3.4.4 Fibers

Early attempts to prepare mesoporous silica fibers employed mechanical drawing[146] or emulsion biphase chemistry.[147] The latter method resulted in fibers with a

Encyclopedia of Inorganic and Bioinorganic Chemistry, Online © 2011 John Wiley & Sons, Ltd.

This article was originally published in the *Encyclopedia of Inorganic Chemistry* in 2006 by John Wiley & Sons, Ltd.
DOI: 10.1002/9781119951438.eibc0264

single-crystal-like mesostructure where the pore channels run circularly around the fiber axis.[148] Recently, Stucky and coworkers reported a simple one-phase route to mesostructured fibers.[149] The most intriguing aspect of this route is that the internal architecture of such nanofibers can be readily controlled via the synthesis.

3.5 Structural Stability

For applications of mesoporous materials, their structural stability is among the most important considerations and has therefore been studied extensively. Cassiers and coworkers[150] systematically investigated the thermal, hydrothermal, and mechanical stabilities of the most well-known mesoporous silicas. They found that the thermal stability is strongly dependent on the silica source and the wall thickness. M41S materials prepared with fumed silica show higher thermal stability than those made from TEOS. Transformation of layered silicates to mesoporous silica allows the resulting porous clay heterostructures (PCH) and FSM-16 to possess more condensed and ordered walls than M41S materials. It is well known that SBA-15 consists of thicker walls, and is thus expected to exhibit good thermal stability. The following stability trend has been observed by Cassiers *et al*.: MCM-41 (fumed silica), MCM-48 (fumed silica), KIT-1 (colloidal silica) > SBA-15(TEOS) > FSM-16 (layered silicate), PCH (layered silicate) > MCM-41 (TEOS), MCM-48 (TEOS), HMS (TEOS).

The hydrothermal stability is mainly dependent on the wall thickness and the degree of polymerization. KIT-1 and SBA-15 are highly resistant to hydrothermal treatment due to their highly polymerized and thicker walls. Under mild steaming conditions, the pore structure might lead to different hydrothermal stability for materials with comparable wall thickness. Cubic MCM-48 exhibits less structural degradation than the hexagonal mesoporous materials. A complete hydrothermal stability order reported by Cassiers *et al*. is as follows: KIT-1 > SBA-15 > MCM-48 (fumed silica and TEOS), PCH > FSM-16, MCM-41 (fumed silica and TEOS), HMS.

Unlike the thermal and hydrothermal stabilities, the mechanical stability seems less dependent on the nature of mesoporous materials. All materials gradually collapse with the increase of pressure, accompanied with the decrease of surface area and pore volume.[151] Recent studies show that cubic SBA-1 and MCM-48 are more mechanically stable than hexagonal mesoporous materials such as MCM-41 and SBA-15.[152] Hydrolysis of Si–O–Si bonds by water adsorbed onto the silanol groups under compression was found as the main reason for mechanical instability.[153] Organically functionalized materials are more hydrophobic than unmodified counterparts, and thus show enhanced mechanical stability due to the water repelling ability.[154]

3.6 Application

Since the discovery of ordered mesoporous materials, researchers have explored many possible applications that can take advantage of the unique compositional or structural features of mesoporous materials. In addition to applications in traditional areas such as catalysis, separation, and ion exchange, new applications that might involve mesoporous materials include stationary phases in HPLC, bio and macromolecular separations, low dielectric constant materials, enzyme immobilization, optical host materials, templates for fabrication of porous carbons, and reactions in confined environments.

3.6.1 Catalysis[155,156]

The potential application in catalysis is one of the most important uses of ordered mesoporous materials. Mesoporous materials can be used as catalysts in either acid or redox catalysis. To help increase acidity, trivalent cations such as Al and B are often incorporated into siliceous mesoporous framework to generate more acid sites. The acidity can also be generated by dispersing heteropoly acids or by grafting organic functional groups onto the surface of mesoporous solids. Many modified MCM-41 type materials have been found to be catalytically active in selected acid-catalyzed processes, However, owing to their disordered framework, mesoporous materials have only moderate acidity. And this limits their applications in petroleum refining and fine chemical synthesis.

For redox catalysis, efforts have been spent on preparing transition metal modified mesoporous materials. These materials are capable of extending the catalytic oxidation chemistry to large molecules. The selective catalytic activity has also been demonstrated, for example, in the oxidation of aromatic compounds by using titanium-containing mesoporous silica (Ti-MCM-41 and Ti-HMS).[157]

In addition to their direct use as catalysts, mesoporous materials are also useful as catalyst supports because of their high surface area, high thermal stability, and low cost. Extensive studies have been done on the preparation and catalytic activity of metals (e.g. Pt, Pd, Ru, Cu) and metal oxides (e.g. TiO_2, VO_x, ZrO_2, Fe_2O_3) supported on ordered mesoporous materials. The impact of mesoporous materials has also been felt in organometallic chemistry, as shown by a new series of composites being made by functionalizing mesoporous materials with organometallic compounds.[158]

3.6.2 Environmental Remediation and Separation

Removal of heavy-metal ions has been a major focus in environmental remediation and cleanup. Various materials, such as activated charcoal, clays, silica gels, and ion-exchange resins have been used as adsorbents. Functionalized mesoporous silicas have recently proved to be a promising or even better alternative.[159,160] Mercier *et al*. prepared a

Encyclopedia of Inorganic and Bioinorganic Chemistry, Online © 2011 John Wiley & Sons, Ltd.

This article was originally published in the *Encyclopedia of Inorganic Chemistry* in 2006 by John Wiley & Sons, Ltd.
DOI: 10.1002/9781119951438.eibc0264

highly effective Hg^{2+} adsorbent by grafting thiol moieties to the framework walls of mesoporous silica, denoted MP-HMS.[159] Because of the uniform and large pore structure, MP-HMS showed an improved access of guest species to the binding sites along with a high loading capacity of 310 mg g^{-1} (1.5 mmol g^{-1}), compared to those made from disordered porous materials, such as silica gel. Concurrently, Feng and coworkers reported a similar heavy-metal ion adsorbent by modifying large-pore MCM-41 with a cross-linked monolayer of mercaptopropylsilane with thiol terminal groups.[160] The resulting adsorbent, functionalized monolayers on mesoporous supports (FMMS), was extremely effective for the removal of Hg^{2+} and other heavy-metal ions. The high relative surface coverage of monolayers (up to 76%) led to a remarkable adsorption capacity of 505 mg g^{-1} for Hg^{2+}. To simplify the synthesis procedure, Mercier *et al.* developed a one-step method by cocondensation of TEOS with 3-mercaptopropyltrimethoxysilane in the presence of surfactants.[161]

Unlike the previously studied mercaptopropyl ligand, the thiourea ligands are expected to have weaker bonding to mercury ions in comparison to thiol group, which should facilitate the adsorbent regeneration.[162] A good example is large-pore MCM-41 grafted with 1-allyl-3-propylthiourea,[163] which could be conveniently regenerated under mild conditions. Recent work in this area has focused on the improvement of mercury adsorption capacity. A logical strategy to increase capacity is the use of multifunctional ligands.[162] Grafting of (1,4)-bis(triethoxysilyl)propane tetrasulfide onto the surface of SBA-15 has led to an adsorbent with an unprecedented loading capacity of 13.5 mmol Hg^{2+} g^{-1}.[164] Functionalized mesoporous silicas for the removal of other metal ions, such as Pb^{2+}, Cu^{2+}, and Zn^{2+}, have also been reported.[165]

3.6.3 Chromatography

Commercial chromatography silica stationary phases were prepared by the polymerization induced colloidal assembly (PICA) method,[166] subsequently exhibiting an interparticle (textural) pore structure with moderate surface area (100–550 m^2 g^{-1}) and broad pore-size distribution. Ordered mesoporous silicas show a high surface area up to 1600 m^2 g^{-1} coupled with tunable and uniform pore size arising from intraparticle (structural) porosity, and are thus expected to provide superior chromatographic performance as stationary phases. MCM-41 was first tested as chromatographic matrix for normal-phase high-performance liquid chromatography (HPLC)[167] and size-exclusion chromatography.[168] The most intriguing advantage of MCM-41 is the ability to separate different types of analytes (basic, acidic, and neutral) with good column efficiency within reasonable analysis times.[167] Gallis *et al.*[169] used acid-prepared mesoporous spheres (APMS) to separate ferrocene from acetylferrocene by normal-phase flash liquid chromatography, exhibiting better separating ability (e.g. longer retention time, higher selectivity) than commercial silicas. Similar results have also been obtained in normal-phase, reversed-phase, and chiral HPLC based on APMS and spherical MCM-48.[170,171] Boissiere and coworkers[172] used MSU-1 spheres to separate polycyclic aromatic hydrocarbons (PAHs) by normal-phase HPLC. Separation of biomolecules was accomplished on spherical SBA-15 by reversed-phase HPLC.[173] In comparison to their applications in HPLC, there are only few efforts to use mesoporous silicas in gas chromatography (GC).[174]

4 MACROPOROUS MATERIALS

4.1 Synthesis

Ordered macroporous materials can be templated by colloidal crystals or emulsions. In comparison to microporous and mesoporous materials, the synthesis strategy of macroporous materials is relatively simple.

4.1.1 Colloidal Crystal Templating

A general three-step procedure[175,176] for the formation of macroporous materials by colloidal crystal templating is illustrated in Figure 6. In the first step, monodispersed colloidal spheres assemble into ordered 3D or sometimes 2D arrays to serve as templates. Secondly, the voids of colloidal crystals are filled by precursors that subsequently solidify to form composites. Finally, the original spheres are removed, creating a solid framework with interconnected voids, which faithfully replicate the template arrays.

Latex and silica spheres are the most commonly used templates for the colloidal crystal assembly, because they are highly monodisperse and commercially available. Many crystallization methods have been used to form close-packed structures, including sedimentation, centrifugation, filtration, convective deposition, slit filling, and pressing. All these methods result in polycrystalline domains, usually with face-centered cubic (fcc) packing or randomly stacked hexagonal close-packed planes (rhcp), affording 26-vol% void space. Sometimes colloidal crystals are sintered or annealed to increase their stability and ensure interconnection.

The design of the interstices filling in colloidal crystals with appropriate media and subsequently fluid–solid transformation is central to the whole synthesis. Fluid precursors in the voids of crystal arrays can solidify by polymerization[177] and sol-gel hydrolysis.[178] More recently, many methods[179] have been developed including salt precipitation and chemical conversion, chemical vapor deposition (CVD), spraying techniques (spray pyrolysis, ion spraying, and laser spraying), nanocrystal deposition and sintering, oxide and salt reduction, electrodeposition, and electroless deposition.

Encyclopedia of Inorganic and Bioinorganic Chemistry, Online © 2011 John Wiley & Sons, Ltd.

This article was originally published in the *Encyclopedia of Inorganic Chemistry* in 2006 by John Wiley & Sons, Ltd.
DOI: 10.1002/9781119951438.eibc0264

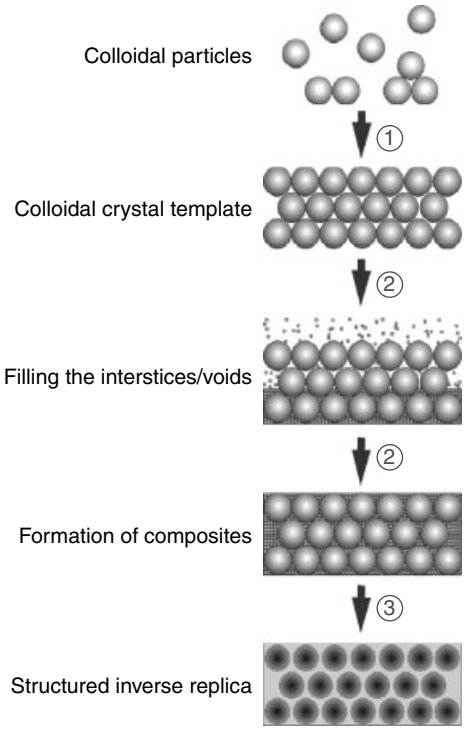

Figure 6 A schematic of the general procedure for preparing ordered macroporous materials by colloidal crystal templating. (1) Assembly of colloidal particles to form colloidal crystal template; (2) Filling the interstices/voids with precursors to form composites; and (3) Removal of templates. (Reprinted from Ref. 175, © 2000, with permission from Elsevier)

Templates should be removed from the composites to yield porous structures. Polymer templates can be removed by calcination, by dissolution with appropriate solvents, or by photo degradation, while silicas are eliminated by dissolution in aqueous HF or NaOH solution.

4.1.2 Emulsion Templating[180,181]

Imhof and Pine have demonstrated that a highly uniform dispersion of emulsion droplets can serve as templates to prepare macroporous materials of titania, silica, and zirconia. In their work, treatment of polydisperse emulsions by shearing and/or fraction resulted in uniform emulsion droplets around which alkoxide precursors are deposited through a sol-gel process. Subsequent drying and heat treatment yielded solid materials with spherical pores left behind by the emulsion droplets (see Figure 7). Macroporous materials templated by emulsion droplets possess highly uniform pores in a wide range from 50 nm to 10 μm, unlike those prepared by colloidal crystal templating whose pore sizes are within 100 to 1000 nm. The materials can be adjusted with any desired porosity up to 90%.

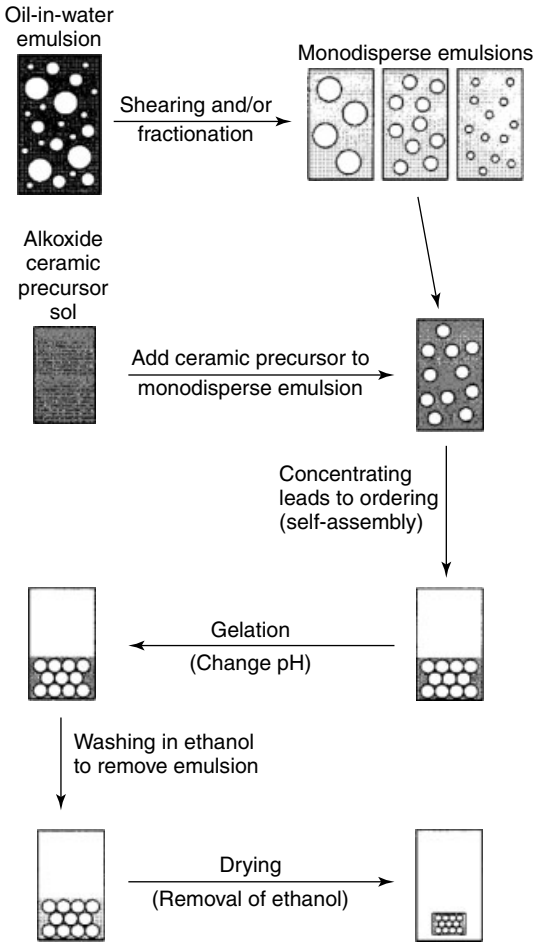

Figure 7 A schematic of procedure to macroporous materials using emulsion droplets as templates. (Reproduced by permission of Wiley VCH)

4.2 Composition and Wall Structures

A summary of ordered macroporous materials with different compositions is given elsewhere.[182,183] Many compositions have been made, ranging from oxides,[177] polymers,[184] and carbons,[185] to semiconductors[186] and metals.[187] The wall structures of macroporous materials can be amorphous, crystalline, with mesopores or micropores, organically modified, or with surface catalysts.[188]

4.3 Applications

Because macroporous materials have 3D periodicity on a length scale comparable to the wavelength of visible light, 3DOM materials have potential use as photonic crystals.[183] Other potential applications include catalysts, bioglasses, sensors, and substrates for surface-enhanced Raman scattering spectroscopy (SERS).[176,179]

Encyclopedia of Inorganic and Bioinorganic Chemistry, Online © 2011 John Wiley & Sons, Ltd.

This article was originally published in the *Encyclopedia of Inorganic Chemistry* in 2006 by John Wiley & Sons, Ltd.
DOI: 10.1002/9781119951438.eibc0264

5 HIERARCHICAL POROUS STRUCTURES

Hierarchical porous materials are solids that are ordered at different length scales. Materials with multiple porosities are of high interest for applications in catalysis and separation, because these applications can take advantages of different pore structures. For example, microporous–mesoporous composites have shown superior catalytic activities by the combination of strong acidity from zeolites with high reactant or product mobility due to large uniform mesopores.[189] Several approaches have been reported on the design and synthesis of hierarchical porous materials, as discussed below.

5.1 Multiple Templating

As discussed previously, organic molecules, supramolecular micelles (or liquid crystals), and colloidal crystals (or emulsions) are employed as templates to prepare microporous, mesoporous, and macroporous materials, respectively. Combining different templates into one synthesis is expected to generate hierarchical porous materials. Yang *et al*. have demonstrated a simple procedure to fabricate hierarchical ordered oxides (silica, niobia, and titania) by concurrently or sequentially combining latex sphere templating, cooperative assembly, and micromolding using polydimethylsiloxane (PDMS) stamps (Figure 8a).[190] In their work, the PDMS mold with micrometer-scale patterns was placed on a substrate, creating accessible channels between the mold and the substrate in which the latex spheres organized into a close-packed array. The voids of the array were filled with a sol-gel block copolymer precursor solution. After sufficient time for cross-linking and polymerization, the mold was removed and the organic templates were eliminated by calcination. The resulting materials exhibited surface patterns of macroporous structures with mesoporous walls (Figure 8, b–e).

Stein and coworkers have synthesized a macroporous silicate with zeolitic microporous frameworks by a 'dual templating' method using latex spheres and tetrapropylammonium hydroxide.[191] Similarly, in situ or simultaneous synthesis of macroporous silica with mesoporous wall[192] and micro/mesoporous composites[193] has been reported in the presence of appropriate dual templates. Microporous/mesoporous materials can also be prepared by a two-step synthetic process, where mesoporous materials are synthesized first, followed by transformation of amorphous mesopore walls into a microporous crystalline (or semicrystalline) phase. Huang *et al*. prepared a MCM-41/ZSM-5 composite containing interconnected mesopore and micropore.[194] Trong On *et al*. demonstrated a general method for the preparation of large-pore mesoporous materials with semicrystalline zeolitic frameworks, involving a templated solid-state secondary crystallization of zeolites from amorphous mesopore walls.[195] Unlike the previous work, Goto and coworkers described a 'reversed' two-step approach to prepare microporous/mesoporous composites using zeolites as the silica-alumina source for mesoporous materials.[196]

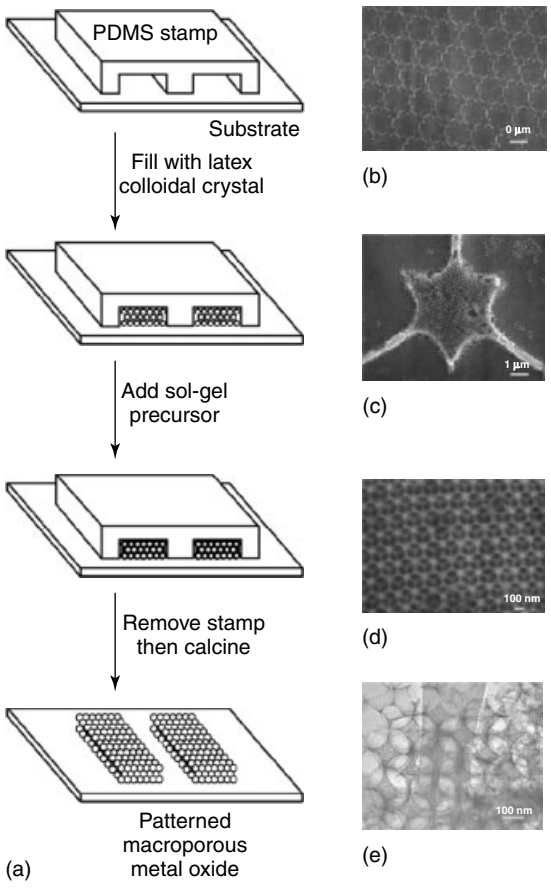

Figure 8 Schematic of the fabrication of hierarchical ordered oxides (a) (Reprinted from Ref. 179, © 2001, with permission from Elsevier) scanning electron microscopy (SEM) images (b, c, d), at different magnifications, of hierarchical ordered mesoporous silica display a high-quality surface pattern (~1000 nm), which is made up of a macroporous (~100 nm) framework of cubic mesoporous silica (~11 nm), as shown in TEM image (e). (Reprinted with permission from P. Yang *et al*., *Science*, 1998, **282**, 2244)

5.2 Assembly from Building Blocks

Colloidal zeolites have been used as building blocks to fabricate hierarchical porous materials. Infiltrating ethanol sol of zeolite nanoparticles into an ordered array of polystyrene spheres resulted in macroporous zeolites, which involves a self-assembly process.[197] After ethanol evaporation, zeolite nanoparticles were aggregated by capillary forces. High concentration of external silanol groups favored the formation of hydrogen bonds between particles and eventually Si–O–Si bonds after calcination. The method has been further developed to produce transparent and self-standing zeolite membranes with controlled mesoporosity.[198] Concurrently, the preformed zeolite-coated polystyrene spheres have been

Encyclopedia of Inorganic and Bioinorganic Chemistry, Online © 2011 John Wiley & Sons, Ltd.

This article was originally published in the *Encyclopedia of Inorganic Chemistry* in 2006 by John Wiley & Sons, Ltd.
DOI: 10.1002/9781119951438.eibc0264

used as building blocks to assemble hierarchical materials with ordered nano, meso, and macroporosity.[199] The core-shell building blocks were fabricated through a 'layer-by-layer' method[200] by alternate adsorption of zeolite nanoparticles and positively charged macromolecules onto latex spheres. This allows the wall thickness of the resulting macroporous monoliths to be fine-tuned by the layer numbers.

5.3 Bulk Dissolution and Structural Rearrangement

The strategy of this method is to utilize the inherent porosity of bulky substrates in the construction of hierarchical structures by incorporating additional pore systems. Diatoms are unicellular algae whose walls are composed of silica with an internal pore diameter at submicron to micron scales. Zeolitization of diatoms, in which zeolite nanoparticles are dispersed on the surface of diatoms followed by a hydrothermal conversation of a portion of the diatom silicas into zeolites, resulted in the formation of a micro/mesoporous composite material.[201] Similarly, wood has also been used as a substrate to prepare meso/macroporous composites and meso/macroporous zeolites. After the synthesis, wood is removed by calcination.[202]

6 RELATED ARTICLES

Self-assembled Inorganic Architectures; Sol–Gel Synthesis of Solids; Zeolites.

7 REFERENCES

1. K. S. W. Sing, D. H. Everett, R. A. W. Haul, L. Moscou, R. A. Pierotti, J. Rouquerol, and R. Siemieniewska, *Pure Appl. Chem.*, 1985, **57**, 603.
2. S. J. Gregg and K. S. W. Sing, 'Adsorption, Surface Area and Porosity', Academic Press, San Diego, CA, 1982.
3. J. D. Joannopoulos, P. R. Villeneuve, and S. Fan, *Nature*, 1997, **386**, 143.
4. Ch. Baerlocher, W. M. Meier, and D. H. Olson, 'Atlas of Zeolite Framework Types', Elsevier, New York, 2001.
5. M. E. Davis, *Nature*, 2002, **417**, 813.
6. N. Zheng, X. Bu, and P. Feng, *Nature*, 2003, **426**, 428.
7. A. Dyer, in 'Encyclopedia of Inorganic Chemistry', ed. B. R. King, John Wiley & Sons, New York, 1994, p. 4364.
8. M. O'Keeffe and O. M. Yaghi, *Chem. Eur. J.*, 1999, **5**, 2796.
9. X. Bu, P. Feng, T. E. Gier, D. Zhao, and G. D. Stucky, *J. Am. Chem. Soc.*, 1998, **120**, 13389.
10. A. Corma, M. J. Diaz-Cabanas, J. Martinez-Triguero, F. Rey, and J. Rius, *Nature*, 2002, **418**, 514.
11. A. K. Cheetham, G. Ferey, and T. Loiseau, *Angew. Chem., Int. Ed. Engl.*, 1999, **38**, 3269.
12. T. E. Gier and G. D. Stucky, *Nature*, 1991, **349**, 508.
13. P. Feng, T. Zhang, and X. Bu, *J. Am. Chem. Soc.*, 2001, **123**, 8608.
14. X. Bu and P. Feng, in 'The Chemistry of Nanostructured Materials', ed. P. Yang, World Scientific, Singapore, 2003, p. 1, and references therein.
15. R. W. J. Scott, M. J. Mac Lachlan, and G. A. Ozin, *Curr. Opin. Solid State Mater. Sci.*, 1999, **4**, 113.
16. N. Zheng, X. Bu, and P. Feng, *Science*, 2002, **298**, 2366.
17. O. M. Yaghi, M. O'Keeffe, N. W. Ockwig, H. K. Chae, M. Eddaoudi, and J. Kim, *Nature*, 2003, **423**, 705.
18. U. Ciesla and F. Schüth, *Micropor. Mesopor. Mater.*, 1999, **27**, 131.
19. F. Di Renzo, A. Galarneau, P. Trens, and F. Fajula, in 'Handbook of Porous Solids', eds. F. Schüth, K. S. W. Sing, and J. Weitkamp, John Wiley & Sons, Weinheim, 2002, p. 1311.
20. C. T. Kresge, M. E. Lonowicz, W. J. Roth, J. C. Vartuli, and J. S. Beck, *Nature*, 1992, **359**, 710.
21. J. S. Beck, J. C. Vartuli, W. J. Roth, M. E. Lonowicz, C. T. Kresge, K. T. Schmitt, C. T.-W. Chu, D. H. Olson, E. W. Sheppard, S. B. McCullen, J. B. Higgins, and J. L. Schlenker, *J. Am. Chem. Soc.*, 1992, **114**, 10834.
22. A. Monnier, F. Schüth, Q. Huo, D. Kumar, D. Margolese, R. S. Maxwell, G. D. Stucky, M. Krishnamurty, P. Petroff, A. Firouzi, M. Janicke, and B. F. Chmelka, *Science*, 1993, **261**, 1299.
23. Q. Huo, D. I. Margolese, U. Ciesla, P. Feng, T. E. Gier, P. Sieger, R. Leon, P. M. Petroff, F. Schuth, and G. D. Stucky, *Nature*, 1994, **368**, 317.
24. Q. Huo, D. I. Margolese, U. Ciesla, D. G. Demuth, P. Feng, T. E. Gier, P. Sieger, A. Firouzi, B. F. Chmelka, F. Schuth, and G. D. Stucky, *Chem. Mater.*, 1994, **6**, 1176.
25. D. Zhao, J. Feng, Q. Huo, N. Melosh, G. H. Fredrickson, B. F. Chmelka, and G. D. Stucky, *Science*, 1998, **279**, 548.
26. D. Zhao, Q. Huo, J. Feng, B. F. Chmelka, and G. D. Stucky, *J. Am. Chem. Soc.*, 1998, **120**, 6024.
27. P. Schmidt-Winkel, W. W. Lukens Jr, D. Zhao, P. Yang, B. F. Chmelka, and G. D. Stucky, *J. Am. Chem. Soc.*, 1999, **121**, 254.
28. P. Schmidt-Winkel, W. W. Lukens Jr, P. Yang, D. I. Margolese, J. S. Lettow, J. Y. Ying, and G. D. Stucky, *Chem. Mater.*, 2000, **12**, 686.
29. P. T. Tanev and T. J. Pinnavaia, *Science*, 1995, **267**, 865.
30. S. A. Bagshaw, E. Prouzet, and T. J. Pinnavaia, *Science*, 1995, **269**, 1242.
31. W. Zhang, B. Glomski, T. R. Pauly, and T. J. Pinnavaia, *Chem. Commun.*, 1999, 1803.
32. D. M. Antonelli and J. Y. Ying, *Angew. Chem., Int. Ed. Engl.*, 1996, **35**, 426.

Encyclopedia of Inorganic and Bioinorganic Chemistry, Online © 2011 John Wiley & Sons, Ltd.

This article was originally published in the *Encyclopedia of Inorganic Chemistry* in 2006 by John Wiley & Sons, Ltd.
DOI: 10.1002/9781119951438.eibc0264

33. D. M. Antonelli, A. Nakahira, and J. Y. Ying, *Inorg. Chem.*, 1996, **35**, 3126.
34. G. S. Attard, J. C. Glyde, and C. G. Goltner, *Nature*, 1995, **378**, 366.
35. P. Feng, X. Bu, and D. Pine, *Langmuir*, 2000, **16**, 5304.
36. C. J. Brinker, Y. Lu, A. Sellinger, and H. Fan, *Adv. Mater.*, 1999, **11**, 579.
37. N. K. Raman, M. T. Anderson, and C. J. Brinker, *Chem. Mater.*, 1996, **8**, 1682.
38. Q. Huo, R. Leon, P. M. Petroff, and G. D. Stucky, *Science*, 1995, **268**, 1324.
39. G. D. Stucky, Q. Huo, A. Firouzi, B. F. Chmelka, S. Schacht, I. G. Voigt-Martin, and F. Schüth, in 'Progress in Zeolite and Microporous Materials, Studies in Surface Science and Catalysis', eds. H. Chon, S.-K. Ihm, and Y. S. Uh, Elsevier, Amsterdam, 1997, Vol. 105, p. 3.
40. Q. Huo, D. I. Margolese, and G. D. Stucky, *Chem. Mater.*, 1996, **8**, 1147.
41. E. Prouzet and T. J. Pinnavaia, *Angew. Chem., Int. Ed. Engl.*, 1997, **36**, 516.
42. A. Sayari, M. Kruk, M. Jaroniec, and I. L. Moudrakovshi, *Adv. Mater.*, 1998, **10**, 1376.
43. D. Khushalani, A. Kuperman, G. A. Ozin, K. Tanaka, J. Garces, M. M. Olken, and N. Coombs, *Adv. Mater.*, 1995, **7**, 842.
44. A. Sayari, Y. Yang, M. Kruk, and M. Jaroniec, *J. Phys. Chem. B*, 1999, **103**, 3651.
45. A. Sayari, *Angew. Chem., Int. Ed. Engl.*, 2000, **39**, 2920.
46. S. S. Kim, W. Zhang, and T. J. Pinnavaia, *Science*, 1998, **282**, 1302.
47. C. Yu, Y. Yu, and D. Zhao, *Chem. Commun.*, 2000, 575.
48. R. Ryoo, J. M. Kim, C. H. Ko, and C. H. Shin, *J. Phys. Chem.*, 1996, **100**, 17718.
49. S. Inagaki, Y. Fukushima, and K. Kuroda, *J. Chem. Soc., Chem. Commun.*, 1993, 680.
50. A. Galarneau, A. Barodawalla, and T. J. Pinnavaia, *Nature*, 1995, **374**, 529.
51. Y. Sakamoto, M. Kaneda, O. Terasaki, D. Zhao, J. M. Kim, G. D. Stucky, H. J. Shin, and R. Ryoo, *Nature*, 2000, **408**, 449.
52. J. R. Matos, M. Kruk, L. P. Mercuri, M. Jaroniec, L. Zhao, T. Kamiyama, O. Terasaki, T. J. Pinnavaia, and Y. Liu, *J. Am. Chem. Soc.*, 2003, **125**, 821.
53. D. Zhao, Q. Huo, J. Feng, J. Kim, Y. Han, and G. D. Stucky, *Chem. Mater.*, 1999, **11**, 2668.
54. J. Y. Ying, C. P. Mehnert, and M. S. Wong, *Angew. Chem., Int. Ed. Engl.*, 1999, **38**, 56.
55. P. Feng, Y. Xia, F. Jiang, X. Bu, and G. D. Stucky, *Chem. Commun.*, 1997, 949.
56. D. Zhao, Z. Luan, and L. Kevan, *Chem. Commun.*, 1997, 1009.
57. B. Tian, X. Liu, B. Tu, C. Yu, J. Fan, L. Wang, S. Xie, G. D. Stucky, and D. Zhao, *Nat. Mater.*, 2003, **2**, 159.
58. P. Yang, D. Zhao, D. I. Margolese, B. F. Chmelka, and G. D. Stucky, *Nature*, 1998, **396**, 152.
59. D. Antonelli and J. Y. Ying, *Angew. Chem., Int. Ed. Engl.*, 1995, **34**, 2014.
60. V. F. Stone Jr and R. J. Davis, *Chem. Mater.*, 1998, **10**, 1468.
61. D. M. Antonelli, *Micropor. Mesopor. Mater.*, 1999, **30**, 315.
62. H. Luo, C. Wang, and Y. Yan, *Chem. Mater.*, 2003, **15**, 3841.
63. J. A. Knowles and M. J. Hudson, *J. Chem. Soc., Chem. Commun.*, 1995, 2083.
64. M. J. Hudson and J. A. Knowles, *J. Mater. Chem.*, 1996, **6**, 89.
65. F. Schueth, *Ber. Bunsen-Ges. Phys. Chem.*, 1995, **99**, 1306.
66. V. Ciesla, S. Schacht, G. D. Stucky, K. K. Unger, and F. Schüth, *Angew. Chem., Int. Ed. Engl.*, 1996, **35**, 541.
67. J. S. Reddy and A. Sayari, *Catal. Lett.*, 1996, **38**, 219.
68. A. Kim, P. Bruinsma, Y. Chen, L.-Q. Wang, and J. Liu, *Chem. Commun.*, 1997, 161.
69. G. Pacheco, E. Zhao, A. Garcia, A. Sklyarov, and J. J. Fripiat, *Chem. Commun.*, 1997, 491.
70. G. Pacheco, E. Zhao, A. Garcia, A. Sklyarov, and J. J. Fripiat, *J. Mater. Chem.*, 1998, **8**, 219.
71. M. S. Wong and J. Y. Ying, *Chem. Mater.*, 1998, **10**, 2067.
72. S. A. Bagshaw and T. J. Pinnavaia, *Angew. Chem., Int. Ed. Engl.*, 1996, **35**, 1102.
73. S. Cabrera, J. El Haskouri, J. Alamo, A. Beltran, D. Beltran, S. Mendioroz, M. D. Marcos, and P. Amoros, *Adv. Mater.*, 1999, **11**, 379.
74. F. J. P. Vaudry, S. Khodabandeh, and M. E. Davis, *Chem. Mater.*, 1996, **8**, 1451.
75. M. Yada, M. Machida, and T. Kijima, *Chem. Commun.*, 1996, 769.
76. Z. Zhang, R. W. Hicks, T. R. Pauly, and T. J. Pinnavaia, *J. Am. Chem. Soc.*, 2002, **124**, 1592.
77. Z. Zhang and T. J. Pinnavaia, *J. Am. Chem. Soc.*, 2002, **124**, 12294.
78. R. Ryoo, S. H. Joo, M. Kruk, and M. Jaroniec, *Adv. Mater.*, 2001, **13**, 677.
79. R. Ryoo, S. H. Joo, and S. Jun, *J. Phys. Chem. B*, 1999, **103**, 7743.
80. J. Lee, S. Yoon, T. Hyeon, S. M. Oh, and K. B. Kim, *Chem. Commun.*, 1999, 2177.
81. S. H. Joo, S. J. Choi, I. Oh, J. Kwak, Z. Liu, O. Terasaki, and R. Ryoo, *Nature*, 2001, **412**, 169.
82. M. Kruk, M. Jaroniec, R. Ryoo, and S. H. Joo, *J. Phys. Chem. B*, 2000, **104**, 7960.
83. S. H. Joo, S. Jun, and R. Ryoo, *Micropor. Mesopor. Mater.*, 2001, **44/45**, 153.
84. J. Lee, S. Yoon, S. M. Oh, C.-H. Shin, and T. Hyeon, *Adv. Mater.*, 2000, **12**, 359.

Encyclopedia of Inorganic and Bioinorganic Chemistry, Online © 2011 John Wiley & Sons, Ltd.

This article was originally published in the *Encyclopedia of Inorganic Chemistry* in 2006 by John Wiley & Sons, Ltd.
DOI: 10.1002/9781119951438.eibc0264

85. S. Jun, S. H. Joo, R. Ryoo, M. Kruk, M. Jaroniec, Z. Liu, T. Hosanna, and O. Terasaki, *J. Am. Chem. Soc.*, 2000, **122**, 10712.
86. M. Kruk, M. Jaroniec, C. H. Ko, and R. Ryoo, *Chem. Mater.*, 2000, **12**, 1961.
87. J. Fan, C. Yu, L. Wang, B. Tu, D. Zhao, Y. Sakamoto, and O. Terasaki, *J. Am. Chem. Soc.*, 2001, **123**, 12113.
88. C. Yu, J. Fan, B. Tian, D. Zhao, and G. D. Stucky, *Adv. Mater.*, 2002, **14**, 1742.
89. S. B. Yoon, J. Y. Kim, and J.-S. Yu, *Chem. Commun.*, 2001, 559.
90. S.-S. Kim and T. J. Pinnavaia, *Chem. Commun.*, 2001, 2418.
91. J.-S. Lee, S. H. Joo, and R. Ryoo, *J. Am. Chem. Soc.*, 2002, **124**, 1156.
92. T.-W. Kim, I.-S. Park, and R. Ryoo, *Angew. Chem., Int. Ed. Engl.*, 2003, **42**, 4375.
93. T. Asia, M. J. Mac Lachlan, N. Coombs, and G. A. Ozin, *Nature*, 1999, **402**, 867.
94. S. Inagaki, S. Guan, Y. Fukushima, T. Hosanna, and O. Terasaki, *J. Am. Chem. Soc.*, 1999, **121**, 9611.
95. B. J. Melded, B. T. Holland, C. F. Branford, and A. Stein, *Chem. Mater.*, 1999, **11**, 3302.
96. T. Asia, G. A. Ozin, H. Grundy, M. Kruk, and M. Jaroniec, in 'Nonporous Materials III, Studies in Surface Science and Catalysis', eds. A. Sayari and M. Jaroniec, Elsevier, Amsterdam, 2002, Vol. 141, p. 1.
97. C. Yeshiva-Ishii, T. Asia, N. Coombs, M. J. Mac Lachlan, and G. A. Ozin, *Chem. Commun.*, 1999, 2539.
98. S. Guan, S. Inagaki, T. Hosanna, and O. Terasaki, *Micropor. Mesopor. Mater.*, 2001, **44–45**, 165.
99. H. Zhu, D. J. Jones, J. Zodiac, J. Rosier, and R. Duarte, *Chem. Commun.*, 2001, 2568.
100. S. Inagaki, S. Guan, T. Hosanna, and O. Terasaki, *Nature*, 2002, **416**, 304.
101. M. J. Mac Lachlan, T. Asia, and G. A. Ozin, *Chem. Eur. J.*, 2000, **6**, 2507.
102. T. Asia, C. Yeshiva-Ishii, M. J. Mac Lachlan, and G. A. Ozin, *J. Mater. Chem.*, 2000, **10**, 1751.
103. F. Bonhomie and M. G. Kanatzidis, *Chem. Mater.*, 1998, **10**, 1153.
104. M. J. Maculation, N. Coombs, and G. A. Ozin, *Nature*, 1999, **397**, 681.
105. K. K. Rang an, S. J. L. Billing, V. Pekoe, J. Heisting, and M. G. Kanatzidis, *Chem. Mater.*, 1999, **11**, 2629.
106. P. N. Realities, K. K. Rang an, and M. G. Kanatzidis, *J. Am. Chem. Soc.*, 2002, **124**, 2604.
107. K. K. Rang an, P. N. Realities, and M. G. Kanatzidis, *J. Am. Chem. Soc.*, 2000, **122**, 10230.
108. K. K. Rang an, P. N. Realities, T. Bakes, and M. G. Kanatzidis, *Chem. Commun.*, 2001, 809.
109. P. N. Realities, T. Bakes, V. Papaefthymiou, and M. G. Kanatzidis, *Angew. Chem., Int. Ed. Engl.*, 2002, **39**, 4558.
110. J. Li, B. Marler, H. Kessler, M. Soulard, and S. Kallus, *Inorg. Chem.*, 1997, **36**, 4697.
111. K. K. Rangan, P. N. Trikalitis, C. Canlas, T. Bakas, D. P. Weliky, and M. G. Kanatzidis, *Nanostruct. Lett.*, 2002, **2**, 513.
112. M. Wachhold, K. K. Rangan, M. Lei, M. F. Thorpe, S. J. L. Billinge, V. Petkov, J. Heising, and M. G. Kanatzidis, *J. Solid State Chem.*, 2000, **152**, 21.
113. P. N. Trikalitis, K. K. Rangan, T. Bakas, and M. G. Kanatzidis, *Nature*, 2001, **410**, 671.
114. P. N. Trikalitis, K. K. Rangan, T. Bakas, and M. G. Kanatzidis, *J. Am. Chem. Soc.*, 2002, **124**, 12255.
115. P. Braun, P. Osenar, and S. I. Stupp, *Nature*, 1996, **380**, 325.
116. G. S. Attard, C. G. Goltner, J. M. Corker, S. Henke, and R. H. Templer, *Angew. Chem., Int. Ed. Engl.*, 1997, **36**, 1315.
117. G. S. Attard, P. N. Bartlett, N. R. B. Coleman, J. E. Elliott, J. R. Owen, and J. H. Wang, *Science*, 1997, **278**, 838.
118. A. H. Whitehead, J. M. Elliott, J. R. Owen, and G. S. Attard, *Chem. Commun.*, 1999, 331.
119. G. S. Attard, S. A. A. Leclerc, S. Maniguet, A. E. Russell, I. Nandhakumar, B. R. Gollas, and P. N. Bartlett, *Micropor. Mesopor. Mater.*, 2001, **44–45**, 159.
120. G. S. Attard, S. A. A. Leclerc, S. Maniguet, A. E. Russell, I. Nandhakumar, B. R. Gollas, and P. N. Bartlett, *Chem Mater.*, 2001, **13**, 1444.
121. S. Guerin and G. S. Attard, *Electrochem. Commun.*, 2001, **3**, 544.
122. S. Pevzner, O. Regev, and R. Yerushalmi-Rozen, *Curr. Opin. Colloid Interface Sci.*, 2000, **4**, 420.
123. M. Ogawa, *J. Am. Chem. Soc.*, 1994, **116**, 7941.
124. M. Ogawa, *Chem. Commun.*, 1996, 1149.
125. I. A. Aksay, M. Trau, S. Manne, I. Honma, N. Yao, L. Zhou, P. Fenter, P. M. Eisenberger, and S. M. Gruner, *Science*, 1996, **273**, 892.
126. H. Yang, A. Kuperman, N. Coombs, S. Mamiche-Afara, and G. A. Ozin, *Nature*, 1996, **379**, 703.
127. Y. Lu, R. Ganuli, C. Drewien, M. Anderson, C. J. Brinker, W. Gong, Y. Guo, H. Soyez, B. Dunn, M. Huang, and J. Zink, *Nature*, 1997, **389**, 364.
128. D. Zhao, P. Yang, D. I. Margolese, B. F. Chmelka, and G. D. Stucky, *Chem. Commun.*, 1998, 2499.
129. H. Yang, N. Coombs, I. Sokolov, and G. A. Ozin, *Nature*, 1996, **381**, 589.
130. A. S. Brown, S. A. Holt, T. Dam, M. Trau, and J. W. White, *Langmuir*, 1997, **13**, 6363.
131. S. Schacht, Q. Huo, I. G. Voigt-Martin, G. D. Stucky, and F. Schuth, *Science*, 1996, **273**, 768.
132. P. C. A. Alberius, K. L. Frindell, R. C. Hayward, E. J. Kramer, G. D. Stucky, and B. F. Chmelka, *Chem. Mater.*, 2002, **14**, 3284.
133. E. L. Crepaldi, G. Jde. A. A. Soler-Illia, D. Grosso, P.-A. Albouy, and C. Sanchez, *Chem. Commun.*, 2001, 1582.

Encyclopedia of Inorganic and Bioinorganic Chemistry, Online © 2011 John Wiley & Sons, Ltd.

This article was originally published in the *Encyclopedia of Inorganic Chemistry* in 2006 by John Wiley & Sons, Ltd.
DOI: 10.1002/9781119951438.eibc0264

134. H. Miyata, M. Itoh, M. Watanabe, and T. Noma, *Chem. Mater.*, 2003, **15**, 1334.

135. K. Landskron, B. D. Hatton, D. D. Perovic, and G. A. Ozin, *Science*, 2003, **302**, 266.

136. S. Schacht, Q. Huo, I. G. Voigt-Martin, G. D. Stucky, and F. Schuth, *Science*, 1996, **273**, 768.

137. Q. Huo, J. Feng, F. Schüth, and G. D. Stucky, *Chem. Mater.*, 1997, **9**, 14.

138. M. Grün, I. Lauer, and K. K. Unger, *Adv. Mater.*, 1997, **9**, 254.

139. G. Büchel, M. Grün, K. K. Unger, A. Matsumoto, and K. Tsutsumi, *Supramol. Sci.*, 1998, **5**, 253.

140. K. Schumacher, M. Grün, and K. K. Unger, *Micropor. Mesopor. Mater.*, 1999, **27**, 201.

141. G. V. Rama Rao, G. P. Lopez, J. Bravo, H. Pham, A. K. Datye, H. Xu, and T. L. Ward, *Adv. Mater.*, 2002, **14**, 1301.

142. T. Martin, A. Galarneau, F. Di Renzo, F. Fajula, and D. Plee, *Angew. Chem., Int. Ed. Engl.*, 2002, **41**, 2590.

143. P. Feng, X. Bu, G. D. Stucky, and D. J. Pine, *J. Am. Chem. Soc.*, 2000, **122**, 994.

144. S. A. El-Safty and T. Hanaoka, *Adv. Mater.*, 2003, **15**, 1893.

145. H. Yang, Q. Shi, B. Tian, S. Xie, F. Zhang, Y. Yan, B. Tu, and D. Zhao, *Chem. Mater.*, 2003, **15**, 536.

146. P. Yang, D. Zhao, B. F. Chmelka, and G. D. Stucky, *Chem. Mater.*, 1998, **10**, 2033.

147. Q. Huo, D. Zhao, J. Feng, K. Weston, S. K. Buratto, G. D. Stucky, S. Schacht, and F. Schüth, *Adv. Mater.*, 1997, **9**, 974.

148. F. Marlow, B. Spliethofff, B. Tesche, and D. Zhao, *Adv. Mater.*, 2000, **12**, 961.

149. J. Wang, J. Zhang, B. Y. Asoo, and G. D. Stucky, *J. Am. Chem. Soc.*, 2003, **125**, 13966.

150. K. Cassiers, T. Linssen, M. Mathieu, M. Benjelloun, K. Schrijnemakers, P. Van Der Voort, P. Cool, and E. F. Vansant, *Chem. Mater.*, 2002, **14**, 2317.

151. N. Bai, Y. Chi, Y. Zou, and W. Pang, *Mater. Lett.*, 2002, **54**, 37.

152. A. Vinu, V. Murugesan, and M. Hartmann, *Chem. Mater.*, 2003, **15**, 1385.

153. T. Tatsumi, K. A. Koyano, Y. Tanaka, and S. Nakata, *J. Porous Mater.*, 1999, **6**, 13.

154. N. Igarashi, K. Hashimoto, and T. Tatsumi, *J. Mater. Chem.*, 2002, **12**, 3631.

155. A. Sayari, *Chem. Mater.*, 1996, **8**, 1840.

156. D. Trong On, D. Desplantier-Giscard, C. Danumah, and S. Kaliaguine, *Appl. Catal., A: Gen.*, 2003, **253**, 545.

157. P. T. Tanev, M. Chibwe, and T. J. Pinnavaia, *Nature*, 1994, **368**, 321.

158. R. Anwander, *Chem. Mater.*, 2001, **13**, 4419.

159. L. Mercier and T. J. Pinnavaia, *Adv. Mater.*, 1997, **9**, 500.

160. X. Feng, G. E. Fryxell, L.-Q. Wang, A. Y. Kim, J. Liu, and K. M. Kemner, *Science*, 1997, **276**, 923.

161. J. Brown, R. Richer, and L. Mercier, *Micropor. Mesopor. Mater.*, 2000, **37**, 41.

162. V. Antochshuk, O. Olkhovyk, M. Jaroniec, I.-S. Park, and R. Ryoo, *Langmuir*, 2003, **19**, 3031.

163. V. Antochshuk and M. Jaroniec, *Chem. Commun.*, 2002, 258.

164. L. Zhang, W. Zhang, J. Shi, Z. Han, Y. Li, and J. Yan, *Chem. Commun.*, 2003, 210.

165. A. M. Liu, K. Hidajat, S. Kawi, and D. Zhao, *Chem. Commun.*, 2000, 1145.

166. R. K. Iler and H. J. McQueston, *U.S. Patent*, 4,010,242, 1977.

167. M. Grün, A. A. Kurganov, S. Schacht, F. Schuth, and K. K. Unger, *J. Chromatogr., A*, 1996, **740**, 1.

168. A. Kurganov, K. Unger, and T. Issaeva, *J. Chromatogr., A*, 1996, **753**, 177.

169. K. W. Gallis, J. T. Araujo, K. J. Duff, J. G. Moore, and C. C. Landry, *Adv. Mater.*, 1999, **11**, 1452.

170. K. W. Gallis, A. G. Eklund, S. T. Jull, J. T. Araujo, J. G. Moore, and C. C. Landry, *Stud. Surf. Sci. Catal.*, 2000, **129**, 747.

171. C. Thoelen, K. Van de Walle, I. F. J. Vankelecom, and P. A. Jacobs, *Chem. Commun.*, 1999, 1841.

172. C. Boissiere, M. Kummel, M. Persin, A. Larbot, and E. Prouzet, *Adv. Funct. Mater.*, 2001, **11**, 129.

173. J. Zhao, F. Gao, Y. Fu, W. Jin, P. Yang, and D. Zhao, *Chem. Commun.*, 2002, 752.

174. M. Raimondo, G. Perez, M. Sinibaldi, A. De Stefanis, and A. A. G. Tomlinson, *Chem. Commun.*, 1997, 1343.

175. O. D. Velev and A. M. Lenhoff, *Curr. Opin. Colloid Interface Sci.*, 2000, **5**, 56.

176. A. Stein, *Micropor. Mesopor. Mater.*, 2001, **44/45**, 227.

177. O. D. Velev, T. A. Jede, R. F. Lobo, and A. M. Lenhoff, *Nature*, 1997, **389**, 447.

178. B. T. Holland, C. F. Blanford, and A. Stein, *Science*, 1998, **281**, 538.

179. A. Stein and R. C. Schroden, *Curr. Opin. Solid State Mater. Sci.*, 2001, **5**, 553.

180. A. Imhof and D. J. Pine, *Nature*, 1997, **389**, 948.

181. A. Imhof and D. J. Pine, *Adv. Mater.*, 1998, **10**, 697.

182. O. D. Velev and E. W. Kaler, *Adv. Mater.*, 2000, **12**, 531.

183. Y. Xia, B. Gates, Y. Yin, and Y. Lu, *Adv. Mater.*, 2000, **12**, 693.

184. S. H. Park and Y. Xia, *Chem. Mater.*, 1998, **10**, 1045.

185. A. A. Zakhidov, R. H. Baughman, Z. Iqbal, C. Cui, I. Khayrullin, S. O. Dantas, J. Marti, and V. G. Ralchenko, *Science*, 1998, **282**, 897.

186. Y. A. Vlasov, N. Yao, and D. J. Norris, *Adv. Mater.*, 1999, **11**, 165.

187. K. M. Kulinowski, P. Jiang, H. Vaswani, and V. L. Colvin, *Adv. Mater.*, 2000, **12**, 833.

Encyclopedia of Inorganic and Bioinorganic Chemistry, Online © 2011 John Wiley & Sons, Ltd.

This article was originally published in the *Encyclopedia of Inorganic Chemistry* in 2006 by John Wiley & Sons, Ltd.
DOI: 10.1002/9781119951438.eibc0264

188. C. F. Blanford, H. Yan, R. C. Schroden, M. Al-Daous, and A. Stein, *Adv. Mater.*, 2001, **13**, 401.

189. A. Corma, V. Fornes, J. Martinez-Triguero, and S. B. Pergher, *J. Catal.*, 1999, **186**, 57.

190. P. Yang, T. Deng, D. Zhao, P. Feng, D. Pine, B. F. Chmelka, G. M. Whitesides, and G. D. Stucky, *Science*, 1998, **282**, 2244.

191. B. T. Holland, L. Abrams, and A. Stein, *J. Am. Chem. Soc.*, 1999, **121**, 4308.

192. Q. Luo, L. Li, B. Yang, and D. Zhao, *Chem. Lett.*, 2000, 378.

193. A. Karlsson, M. Stocker, and R. Schmidt, *Micropor. Mesopor. Mater.*, 1999, **27**, 181.

194. L. Huang, W. Guo, P. Deng, Z. Xue, and Q. Li, *J. Phys. Chem. B*, 2000, **104**, 2817.

195. D. Trong On and S. Kaliaguine, *Angew. Chem., Int. Ed. Engl.*, 2001, **40**, 3248.

196. Y. Goto, Y. Fukushima, P. Rath, Y. Imada, Y. Kubota, Y. Sugi, M. Ogura, and M. Matsukata, *J. Porous Mater.*, 2002, **9**, 43.

197. L. Huang, Z. Wang, J. Sun, L. Miao, Q. Li, Y. Yan, and D. Zhao, *J. Am. Chem. Soc.*, 2000, **122**, 3530.

198. L. Huang, Z. Wang, H. Wang, J. Sun, Q. Li, D. Zhao, and Y. Yan, *Micropor. Mesopor. Mater.*, 2001, **48**, 73.

199. K. H. Rhodes, S. A. Davis, F. Caruso, B. Zhang, and S. Mann, *Chem. Mater.*, 2000, **12**, 2832.

200. F. Caruso, R. A. Caruso, and H. Mohwald, *Science*, 1998, **282**, 1111.

201. M. W. Anderson, S. M. Holmes, N. Hanif, and C. S. Cundy, *Angew. Chem., Int. Ed. Engl.*, 2000, **39**, 2707.

202. A. Dong, Y. Wang, Y. Tang, N. Ren, Y. Zhang, Y. Yue, and Z. Gao, *Adv. Mater.*, 2002, **14**, 926.

Encyclopedia of Inorganic and Bioinorganic Chemistry, Online © 2011 John Wiley & Sons, Ltd.

This article was originally published in the *Encyclopedia of Inorganic Chemistry* in 2006 by John Wiley & Sons, Ltd.
DOI: 10.1002/9781119951438.eibc0264